ACS OMEGA

http://pubs.acs.org/journal/acsodf

Article

Synergistic Efficiency of Zinc Oxide/Montmorillonite Nanocomposites and a New Derived Saponin in Liquid/Liquid/Solid Interface-Included Systems: Application in Nanotechnology-Assisted Enhanced Oil Recovery

Ahmad Nourinia, Abbas Khaksar Manshad,* Seyed Reza Shadizadeh, Jagar A. Ali, Stefan Iglauer, Alireza Keshavarz, Amir H. Mohammadi,* and Muhammad Ali

Cite This: *ACS Omega* 2022, 7, 24951−24972

Read Online

ACCESS | Metrics & More | Article Recommendations | Supporting Information

ABSTRACT: Oil production faces challenges such as limited oil production from carbonate reservoirs, high oil production costs, and environmental issues. Chemical flooding as an enhanced oil recovery (EOR) method (CEOR) can increase oil production by the use of chemical additives such as surfactants into the reservoirs. Surfactants can increase oil recovery by interfacial tension (IFT) reduction and alteration of the rock wettability from oil-wet to water-wet. The synthesis of chemicals such as synthetic surfactants is usually costly and harmful to the environment. To solve these problems, many researchers have oriented on the use of natural surfactants instead of synthetic ones within the CEOR process. A new approach to increase the efficiency of CEOR is the synergizing of the chemical additives with nanoparticles as a hybrid fluid, which is known as the nanotechnology-assisted EOR method. In this research, a natural surfactant derived from *Cyclamen persicum* (CP) plant was extracted, and its performance was optimized with the zinc oxide/montmorillonite (ZnO/MMT) nanocomposite in a synergistic usage. At the optimum concentration of the surfactant, the measurements of the IFT and the contact angle show 57.78 and 61.58% optimizations, respectively. Also, in the presence of NaCl, the performance of CP is improved. IFT and contact angle measurements were also conducted for ZnO/MMT nanofluids and CP-ZnO/MMT as hybrid nanofluids. Results indicate that ZnO/MMT nanocomposites can alter the wettability of the carbonate rock to the water-wet state. Also, the CP-ZnO/MMT hybrid nanofluid shows a good potential in both IFT reduction and altering wettability from oil-wet to water-wet. Finally, to investigate the effects of solutions on increasing oil recovery factor (RF), the optimum concentrations of the surfactant, nanocomposite, and hybrid solutions were selected for dynamic core flooding experiments, and improvements showed oil RF increases of 8.2, 6, and 13%, respectively.

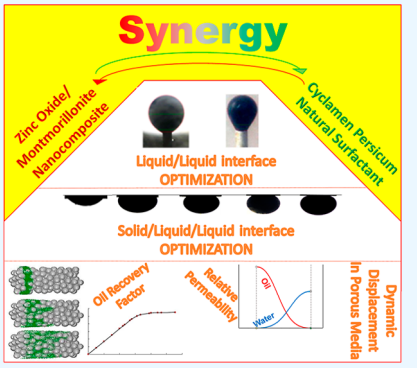

1. INTRODUCTION

Due to declining oil reserves, oil extraction methods are constantly being improved. One of the enhanced oil recovery (EOR) methods is chemical injection defined as chemical enhanced oil recovery (CEOR), which includes injecting chemical additives such as surfactants, polymers, alkalis, and the combination of them into the reservoir.

The main mechanism of surfactants to increase oil production is interfacial tension (IFT) reduction.[1] In some cases, the surfactants have shown their ability to alter the wettability of reservoir rock.[2] In terms of surfactant types, they are typically divided into two categories: synthetic and natural surfactants.[3]

The use of synthetic surfactants in the petroleum industry faces challenges. The high production cost of synthetic surfactants can make the EOR process economically impossible. On the other hand, environmental and human hazards due to the use of chemical surfactants are unavoidable. Corrosion of equipment and toxicity of the environment as a result of the use of the ionic surfactants are examples of these hazards.[4] One of the solutions to overcome these challenges is the use of natural surfactants, which has been considered by many researchers in recent years. Due to the saponin content of natural surfactants, they are known as nonionic surfactants.[5] Table S1 shows examples of the natural surfactants and their plant sources. Unfortunately, natural surfactants do not work well compared to synthetics. One of the reasons for the poor performances of natural surfactants could be mentioned as the presence of impurities in elementary laboratory plant extracts.

Nanoparticles can be used in the CEOR methods as a hybrid agent to improve the performances of the additives, which is

Received: December 20, 2021
Accepted: June 23, 2022
Published: July 15, 2022

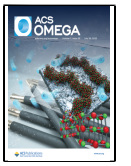

https://doi.org/10.1021/acsomega.1c07182
ACS Omega 2022, 7, 24951−24972

known as the nanotechnology-assisted enhanced oil recovery (NEOR) method.[6] The target of using new additives in CEOR is satisfaction with the mechanisms applied in enhancing the recovery of oil that could mainly be mentioned as mobility control improvement, IFT reduction, and wettability alteration. Used chemicals in CEOR have to sustain the harsh conditions of hydrocarbon reservoirs; therefore, the properties of certain additives should not be altered by the changes in conditions. Nanotechnology acts here as an intensifier in enhancing the properties and will make a synergistic effect with used additives. Recently, many studies have been conducted on the use of nanotechnology as a synergy with surfactants to improve their performances. The use of nanoparticles with surfactants as a hybrid fluid improves the performances of some surfactants for EOR applications.[7] Nanoparticles, for example, can overcome the weakness of surfactants in wettability alteration and cause a higher oil recovery factor (RF).[8−10] However, the mechanisms of nanosurfactant hybrids are not yet entirely understood, and complementary studies are continuing.

Chhetri et al. introduced a natural surfactant prepared from the *Sapindus mukurossi* fruit, and this surfactant can reduce IFT.[11] Pordel Shahri et al. investigated the effect of the *Ziziphus spina-christi* (ZSC) leaf extract on IFT. This surfactant decreases the IFT value from 48 to 9 mN/m.[12] Deymeh et al. investigated the effect of the *Seidlitzia rosmarinus* extract on IFT reduction. The extract decreases the IFT from an initial value of 32 to 9 mN/m at critical micelle concentration (CMC).[13] Ahmadi et al. investigated the effect of the *mulberry* leaf extract on IFT reduction and oil recovery. The recorded data indicate that the extract reduces the IFT from 44 to 17.9 mN/m. Based on the core flooding experiment results, the natural surfactant can increase the oil recovery from 49 to 66.8%.[14] Rahmati et al. compared the effect of the mulberry leaf extract with a natural surfactant named *henna* on IFT and wettability alteration. Based on the obtained results, the henna extract shows a better performance to reduce the IFT and contact angle of the oil with a sandstone rock.[15] Emadi et al. investigated the effects of ZSC and silica nanoparticles on the IFT and RF. The results of IFT measurement show that the ZSC can reduce the IFT, and adding silica nanoparticles to the CMC of ZSC reduces the IFT more. Also, by adding nanosilica to ZSC, the RF increases from 53 to 74% of the ordinary oil in place (OOIP).[16] Xu et al., Cheraghian et al., Haeri et al., Songolzadeh and Moghadasi, Zhao et al., and Zhong et al. have shown that the combinations of silica nanoparticles with different surfactants have a good potential to alter wettability from oil-wet to water-wet.[17−22] Suleimanov et al. showed that nonferrous metal NPs can reduce IFT/surface tension.[23] Mohajeri et al., by combining ZrO_2 NPs with sodium dodecyl sulfate and CTAB, showed that the nanofluids optimize IFT/surface tension and alter wettability.[24] Table S2 summarizes the studies on the synergistic effects of nanosurfactants.[17−29]

There is not enough information in the field of studying the mechanisms of IFT reduction, wettability alteration, and oil displacement of natural surfactants and their synergy effects in the presence of nanoparticles. Therefore, in the present study, after extracting a natural surfactant solution from a saponin-containing plant, its synergistic effects were studied together with a green nanocomposite. Both the natural surfactant and synthesized nanocomposite are novel and have not yet been studied in the field of EOR.

In this study, the researchers intended to investigate the effect of the *Cyclamen persicum* (CP) plant extract as a natural surfactant on the increasing oil recovery. Thermogravimetric (TGA) and Fourier transform infrared spectroscopy (FT-IR) analyses were applied to characterize the extracted solution. To obtain the CMC of the extracted surfactant, electrical conductivity, pH, IFT, and wettability alteration methods were used. Pendant drop and contact angle methods were used to investigate the IFT and wettability alteration, respectively. The ZnO/montmorillonite (ZnO/MMT) nanocomposite that was synthesized in a green manner was analyzed as an EOR agent by the pendant drop and contact angle methods too. FTIR, X-ray diffraction (XRD), and field emission scanning electron microscopy (FE-SEM) analyzes were accomplished to characterize the synthesized matter as a nanocomposite. Then, the nanocomposite combined with the surfactant as a hybrid agent. To study the synergistic effects of the nanocomposite and surfactant, different concentrations of the nanocomposite were mixed with CMC of surfactant solution as the base fluid. Finally, proper concentrations of the surfactant, nanocomposite, and hybrid solutions were selected to study the additional oil recovery by core flooding experiment.

2. MATERIALS AND METHODS

2.1. Materials. *2.1.1. Aqueous Phase.* Double-deionized water (DDW) with ultralow electrical conductivity was used to prepare aqueous solution for the natural surfactant and nanofluid solutions with different concentrations of CP and ZnO/MMT, respectively. Seawater from the Persian Gulf with a pH of 7.67 was used in this study as brine solution in the dynamic fluid flooding process. The composition of prepared seawater is illustrated in Table S3. The used salt of sodium chloride for ion engineering analysis of aqueous solutions was purchased from Merck with 99% purity.

2.1.2. Oil Phase. The crude oil used in this study was prepared from Iranian oil fields and used in the aging process of rock core plugs and rock pellets, IFT measurements, wettability alteration tests, and dynamic oil injections into the core plug. The oil density is 0.89 and 0.771 gr/cm^3 under ambient and reservoir conditions, respectively. Table S4 presents the composition of the used crude oil. The obtained crude oil was filtered by a 5 μm mesh before applying wettability alteration, IFT, and core flooding experiments for the prevention of any undesirable plugging.

2.1.3. Natural Surfactant. CP is a rich saponin plant, in which the tuber part contains saponin.[30] Figure S1 shows the structure of the CP extract.[31] After preparing the CP plants, their tubers were separated from the plants, cleaned and cut into small pieces, and dried under ambient conditions. The prepared tubers (100 g) with 350 ml of DDW were placed in the Soxhlet extractor apparatus for 15 h until a saponin-rich solution was obtained in the chamber of the Soxhlet extractor. After that, to remove solids, the obtained solution was filtered with a laboratory steel cone sieve. The vacuum rotary evaporation method with the water bath set at 50 °C was used to remove water from the filtrate blend. Vacuum conditions cause evaporation to occur at much lower temperatures than the boiling temperature under normal conditions and prevent the degradation of the molecules of the surfactant. The evaporation process continued until 80% volumetric percent of the solution was produced. This volumetric ratio was considered in the manufacture of natural surfactant solutions with various concentrations of the extract.

https://doi.org/10.1021/acsomega.1c07182
ACS Omega 2022, 7, 24951−24972

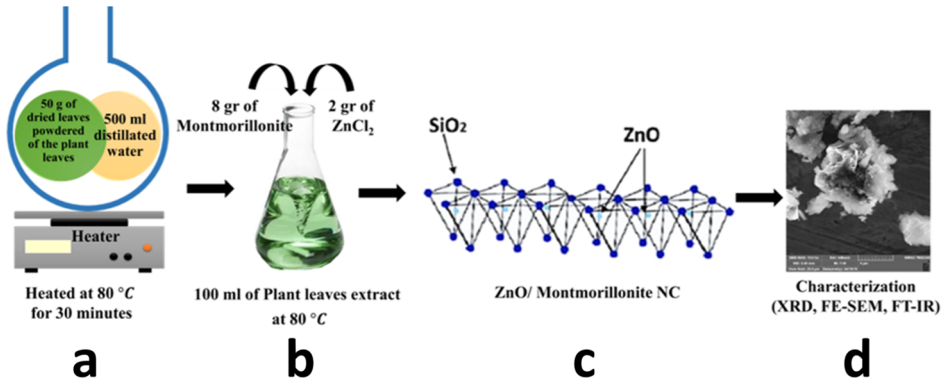

Figure 1. Biosynthesis process of ZnO/MMT nanocomposites (a–d show the steps of the procedure).

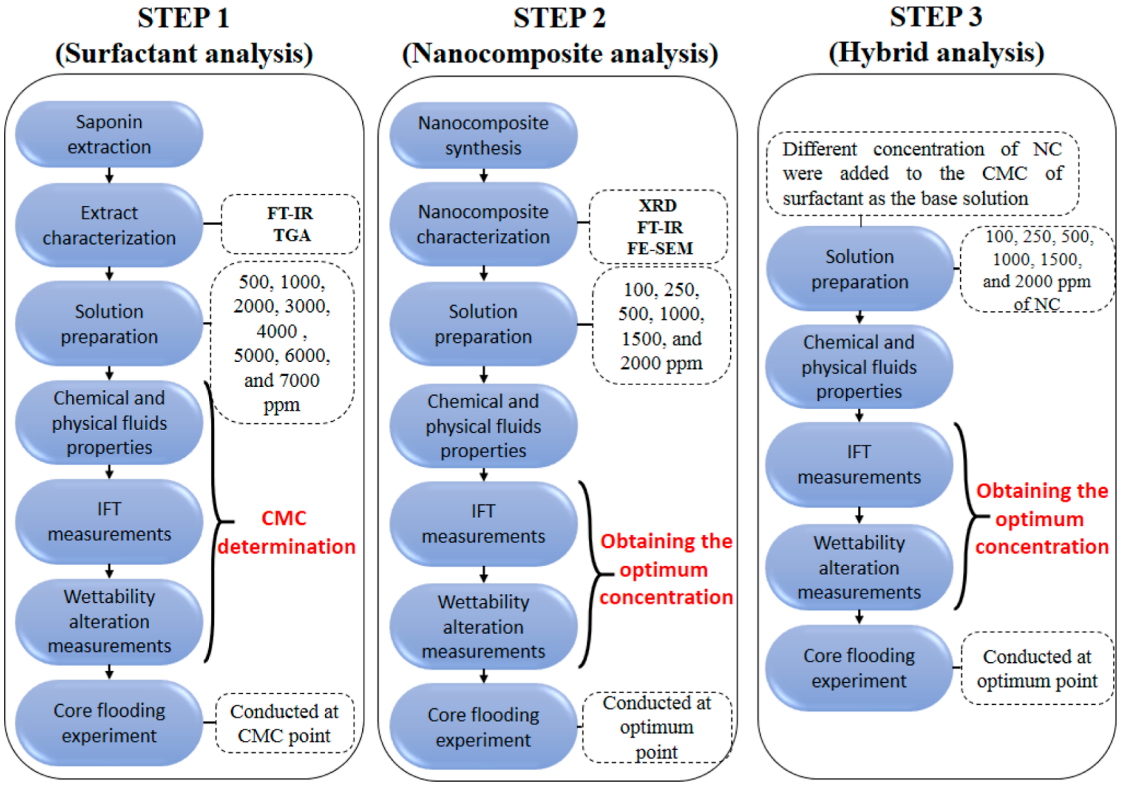

Figure 2. General road map of the present study with details of each step.

2.1.3.1. Characterization of the Natural Surfactant. Even though the literature in medicinal subjects introduces the CP plant extract as a saponin-rich mixture,[32,33] there is no study on the use of this extract in EOR. Therefore, further characterizations were required to approve the presence of saponin and to confirm the successful extraction. FTIR spectroscopy (Bruker Tensor II), in the 400–4000 cm^{-1} wavenumber range, was used to identify the functional group of the extract. TGA was conducted to show the thermal degradation of the natural used extract for a temperature range of 25 to 300 °C. The thermal degradation durability and value of degradation of the extracted material within 25 to 90 °C could also be considered as the thermal stability of the surfactant under general reservoir conditions.

2.1.4. Nanocomposite. In this study, the ZnO/MMT nanocomposite was synthesized as the nanofluid and hybrid agent. From the literature, ZnO nanoparticles can increase the adsorption of MMT on interfaces, and the performance of the MMT is improved in altering the wettability in comparison to MMT individually at solid/liquid/liquid interfaces. The improvement in adsorption can be related to additional active sites that are created by ZnO nanoparticles between the MMT layers. Another reason for improving MMT adsorption phenomena is the increase in the surface area by sited ZnO nanoparticles.[34] Due to the economics and cheapness of MMT, it was decided to use this substance in large quantities and the amount of ZnO by less than half of the whole material.

2.1.4.1. Preparation of the Plant Extract as the Eco-friendly Reducing–Stabilizing Agent. *Ageratum conyzoides* L, a plant of Asteraceae plant family, was used as the eco-friendly agent to provide the reducing media and stabilize the synthesized environment. The potent antioxidant content of the plant strongly confirms the application of its extract as a stabilizing and bioreducing agent for the green synthesis of ZnO/MMT nanostructures.[35,36]

https://doi.org/10.1021/acsomega.1c07182
ACS Omega 2022, 7, 24951–24972

Dried powder (50 g) of the plant leaves was mixed with 500 mL of DDW at 80 °C for 30 min under reflux conditions. The gained extract was monitored using a UV−vis spectrophotometer during the different time intervals to study its stabilization and resistance against decomposition and deformation processes.

2.1.4.2. Synthesis of ZnO/MMT Nanocomposites When Applied in an Environmentally Friendly Manner. The prepared *A. conyzoides* L plant extract (100 mL) was placed within a beaker of 250 cm^3 volume to provide the stabilized reducing medium of synthesis. Chemical powders of zinc chloride and microscopic crystals of MMT phyllosilicates were then added to the reducing environment for 2 and 8 g, in turn. To increase the chemical reaction role-in surfaces, the solution was continuously stirred; also, to increase the reaction rate, the temperature increased to 80 °C and was kept constant. The used synthesized method was the precipitation method; therefore, the stirring process continued until a white precipitate was formed within the system. The precipitated materials were then screened from the synthesized environment through the filtration process. The product went under a 100 °C heating process and washing with DDW for any elimination of purity inclusions. Figure 1 illustrates the biosynthesis process of ZnO/MMT nanocomposites.

2.1.5. Carbonate Core Sample. The carbonate rock sections were obtained from an *Asmari* outcrop located in the south of Iran. The sections were cut into both the cylindrical core plug and circular pellet state of use for dynamic fluid displacement in porous media and wettability alteration experiments, respectively. Circular pellets were polished and divided into four sections to be applicable in the wettability experimental device because of the limitation of visual cell dimensions and use of the contact angle measurement method. Obtained core plugs and circular pellets were then rinsed through a cyclic hydrophilic−lipophilic washing procedure of DDW−acetone−toluene−acetone−DDW to eliminate any probability of dust, precipitated salts, available oleic matters, and other impurities. These unwanted inclusions (if the washing procedure was not applied to the samples) could affect the process as new materials when liquid/liquid and solid/liquid interfacial phenomena were happening and induce errors in measurements.

Induced wettability alterations caused by the presence of different solvents in the samples were not affected during the experiments because the aging processes for gaining a strong oil wetting state were conducted on all the samples.

XRD was conducted on the used sample to determine the composition of the rock. Results of the XRD analysis shows that the used rock type is approximately pure carbonate and contains a high percentage of calcite. Figure S2 shows the result of the XRD test for the prepared rock.

2.2. Methods. Figure 2 illustrates all the steps of the present study. In the first step, it is necessary to characterize the prepared materials to ensure the correct saponin extraction. To evaluate the thermal stability and also to determine functional groups of the natural surfactant, TGA and FT-IR tests were applied on the extracted material, respectively. Surfactant solutions were prepared with 500 to 7000 ppm concentrations of the extract. Electrical conductivity, pH, IFT, and contact angle measurements were used to obtain the CMC of the surfactant. After determining the CMC, the performance of the surfactant at CMC was evaluated in the presence of NaCl. At the end of the first step, the core flooding experiment was applied with the most appropriate concentration of the surfactant and salinity. In the second step, the synthesized nanocomposite is characterized by FT-IR, XRD, and FE-SEM tests to determine functional groups, nanocomposite components, and morphology, respectively. Then, solutions with concentrations of 100, 250, 500, 1000, 1500, and 2000 ppm of the nanocomposite were prepared. After measuring the physical and chemical properties of the prepared solutions, IFT and wettability alteration tests were performed. Finally, the core flooding experiment was conducted at the optimal concentration of nanocomposites, which was obtained from the IFT and wettability alteration tests. In the third step, surfactant solution at CMC was used as the base solution and different concentrations of the nanocomposite were added to it. As in the previous two steps, after measuring the solution properties, the IFT and wettability alteration tests were performed. Finally, the optimal concentrations of hybrid solutions, which were obtained from the IFT and wettability alteration tests, were used as the selected EOR solution in the core flooding experiments.

2.2.1. IFT Measurements. In this study, the pendant drop method was used to calculate the IFT between oil and investigated solutions. The reason for using this method is its accuracy and simplicity.[36,37] In this method, a camera takes pictures from pendant oil droplets and calculates the IFT/surface tension using the below-mentioned equation[36,37]

$$\gamma = \frac{\Delta\rho .\, g .\, D}{H}$$

where γ is the IFT (mN/m^2), $\Delta\rho$ is the difference between the density of the drop and bulk phase (g/cm^3), g is the earth gravitational acceleration (cm/s^2), D is the largest diameter of the droplet (cm), and H is the shape factor of the droplet. The *VIT 6000* apparatus designed by *Fars EOR technologies* was used for both IFT and contact angle measurements. The schematic of the apparatus used in this study is shown in Figure S3. All measurements of IFT were performed under ambient conditions and different concentrations of CP (500 to 7000 ppm) as the basis of hybrid solution and different concentrations of nanocomposites (100, 250, 1000, 1500, and 2000 ppm) used as the hybrid agent.

2.2.2. Wettability Tests. The sessile drop method was utilized to study the wettability alteration of the carbonate rock. Yang's relation for an oil droplet in equilibrium with the rock surface is given below[38]

$$\sigma_{so} = \sigma sw + \sigma_{ow} \cos\theta_{ow}$$

where σ_{so} is the tension between the oil and solid rock surface, σ_{sw} is the tension between the water and solid rock surface, σ_{ow} is the tension between oil and water surfaces, and θ_{ow} represents the contact angle of the droplet that is attached to the rock surface. Given this relation, if the contact angle is less than 90°, the tension between the rock and the oil is low, so the rock is water-wet. If the contact angle is 90°, the water and oil stresses are equal, and the wettability is mediate. Also, if the contact angle is above 90°, the tension between the rock and oil is high and it is an oil-wetted state.[39]

The *VIT6000* was also used to calculate the contact angle between the oil droplets and carbonate surface by the sessile drop method in the presence of CP and hybrid solutions as the medium. Figure S3 shows the schematic of the utilized apparatus. The carbonate rocks are not oil-wet generally; therefore, to achieve the oil-wet system and study the effects of

https://doi.org/10.1021/acsomega.1c07182
ACS Omega 2022, 7, 24951−24972

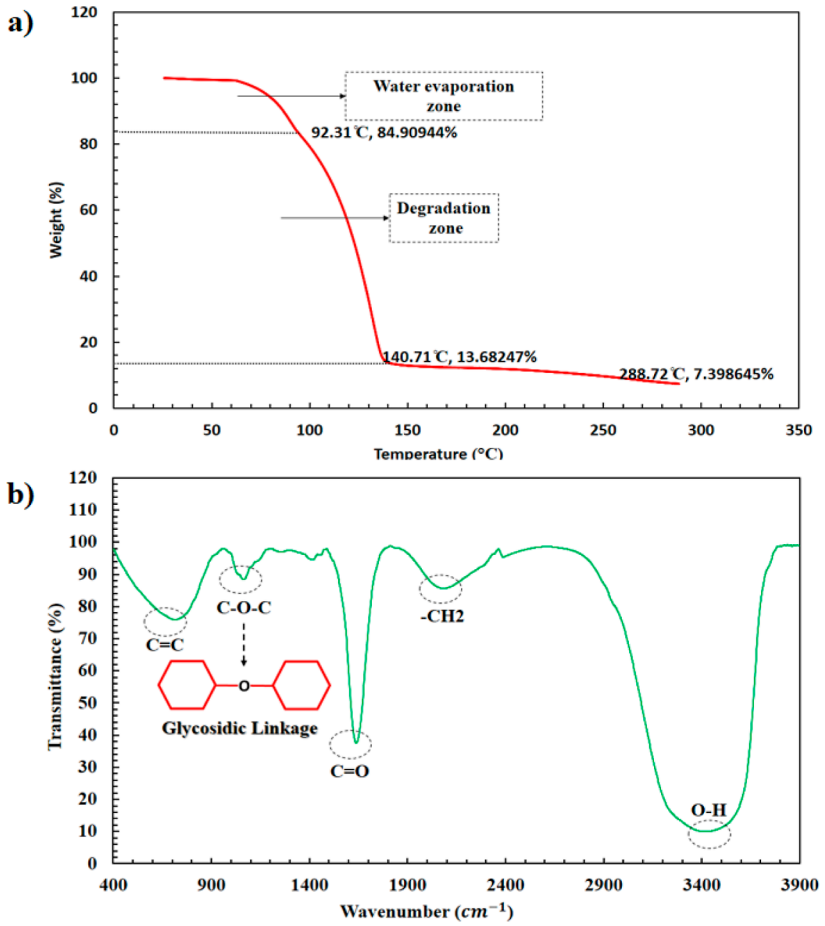

Figure 3. Characterizations of the CP: (a) TGA analysis and (b) FT-IR analysis.

CP and hybrid solutions on wettability alteration, the smooth pellet was immersed in crude oil at 70 °C for 15 days to be aged with oil-wetting agents of the crude oil. During this aging time, the polar components of crude oil adhere onto the surface of the carbonate rock, and they designate a lipophilic or hydrophobic layer on the surface. This prepared lipophilic layer causes a strong oil-wetting state for the surface of the carbonate rock and mimics the original condition of a reservoir oil-wet rock.

In the sessile drop method, the sessile drop is released and placed on the surface, and causes a competition between the oil phase and aqueous phase to adhere on the solid surface. Therefore, the equilibrium of this system requires a minimum time to reach this. Regarding the literature, different times are reported as the equilibrium time which ranged from minutes to hours; therefore, we choose the maximum time of the reported equilibrium to reach it. Consequently, then, each oil-wet pellet was immersed in the selected concentrations of CP and hybrid solutions for 24 h to observe their effects on the wettability alteration in an equilibrium reached state with the sessile drop method of measurement.

2.2.3. Core Flooding Procedure. The core flooding experiments were applied to measure the increase in oil RF by the CP and ZnO/MMT-CP as hybrid solutions at nominated optimal concentrations. A core-flood device made by Fars EOR Technologies Company located in the Abadan Faculty of Petroleum was used to perform the dynamic core flooding tests. In addition to calculating the increase in oil recovery, the porosity and pore volume (PV) of the cores are measured by this device. All the flooding experiments were performed with a flow rate of 0.2 cm^3/min. First, the core was saturated with seawater. Then, by subtraction the dry weight of the cores from the weight of saturated cores, the PV is obtained using the below equation

$$\text{pore volume (CC)} = \frac{\text{saturated weight} - \text{dry weight}}{\text{fluid density}}$$

After obtaining the amount of PV, the oil was then injected into the core to obtain irreducible water saturation (Swirr). To achieve Swirr, the oil injection continued until water production from the core was stopped. The cumulative amount of extracted water from the core was considered as the OOIP, and the below equation was used to calculate irreducible water saturation

$$\text{Swirr (\%)} = \frac{\text{PV} - \text{total extracted water}}{\text{PV}}$$

After reaching the Swirr, the first recovery phase begins with the injection of seawater to the core. This recovery phase is designed to be conducted on the oil-saturated rock plug with including irreducible water saturation and resembles the situation of real secondary oil flooding and acts as a basis for comparison of proposed EOR methods. During the injection of seawater into the core, the differential pressure and accumulative PV injection information were recorded through a differential-pressure transmitter and a hydraulic pump, in turn. The injection of seawater was continued until there was

https://doi.org/10.1021/acsomega.1c07182
ACS Omega 2022, 7, 24951−24972

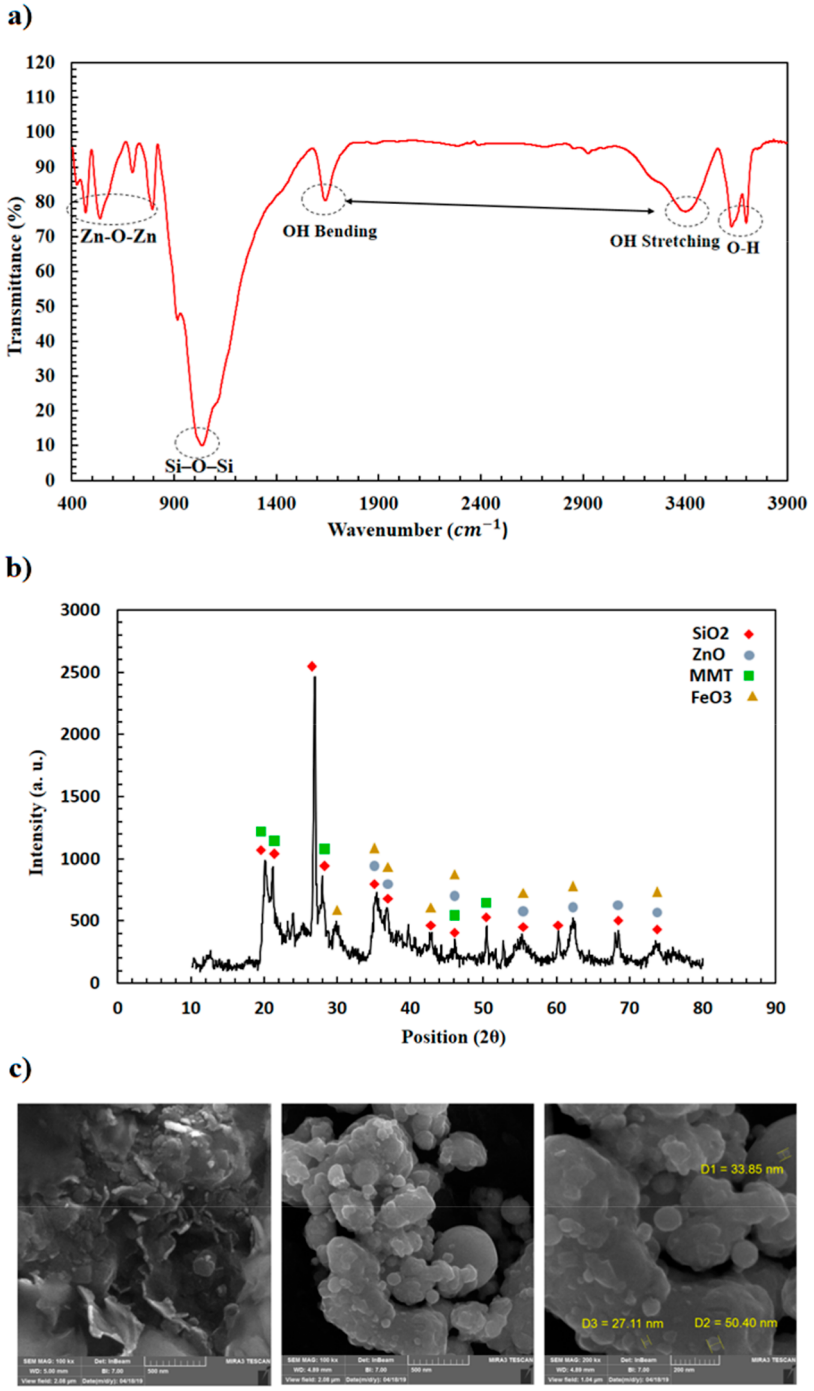

Figure 4. Characterizations of the nanocomposite: (a) FT-IR analysis, (b) XRD test, and (c) FE-SEM analysis.

no more oil production. Finally, the following equation was used to calculate the oil recovery of the first recovery phase

$$\text{RF seawater injection (\% OOIP)} = \frac{\text{oil production in seawater injection}}{\text{original oil in place}}$$

To investigate the effectiveness and impacts of both IFT reduction and wettability alteration toward water wetness by surfactant and hybrid solutions and the ion engineering process, two dynamic displacement experiments were designed to be applied under the same conditions. The first flooding scenario is to observe the effectiveness of ion engineering to the optimum state of the surfactant (CMC), and the second flooding scenario is to investigate the effect of the hybrid state of use of ZnO/MMT with the optimum state of the surfactant (CMC). It should be noted that two designed scenarios were conducted on two similar rock plugs with the same saturation and primary productions.

Just like the first recovery phase, in the second recovery phase, the injections were applied and the pressures and PV injections were recorded. Finally, the increase in oil RF was calculated using the following equation

https://doi.org/10.1021/acsomega.1c07182
ACS Omega 2022, 7, 24951−24972

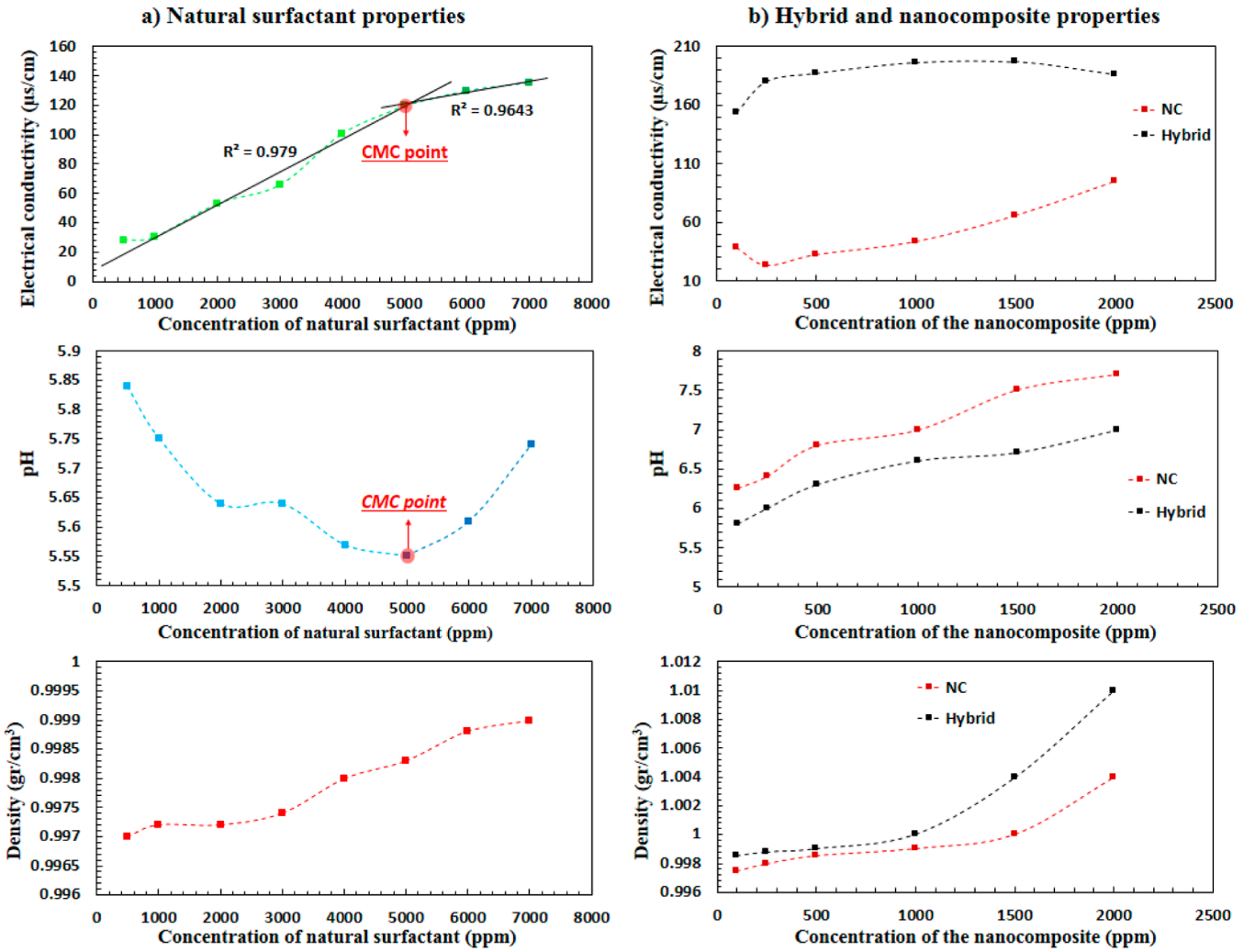

Figure 5. Properties of the solutions: (a) natural surfactant solution and (b) hybrid and nanocomposite solutions.

$$\text{RF surfactant/hybrid injection (\% OOIP)} = \frac{\text{oil production in surfactant/hybrid injection injection}}{\text{original oil in place}}$$

Figure S4 shows the scheme of the dynamic core flooding device made by Fars EOR Technologies. The required force for precise injection of fluids into the porous medium is governed by a hydraulic pump with high accuracy in injection rates. Accumulators are based on the accumulation and injection of different fluids with different scenarios at different times; also, they act as transfer vessels to inject fluids into the core holder to be injected to the porous medium.

A core holder of the Hassler type is applied with a system of the overburden pressure simulator to mimic a semirealized condition. During the conduction of the dynamic displacement test, the differential pressure transmitter records the difference of injection and production pressures to govern the breakthrough and other information. Simultaneous measurement of effluent fluid volumes, displaced volumes, and differential pressures shows the efficiency of each scenario, and the comparison between different scenarios and injection steps is available.

3. RESULTS AND DISCUSSION

3.1. Characterization of the CP Extract. Figure 3a illustrates the TGA test results for CP. In this test, the weight loss of the material was calculated versus temperature. In the presented results, three weight loss zones are observed. The first zone that occurred at ambient to 96.5 °C is related to water evaporation with an 18.22% weight loss. The second degradation zone from 96.5 to 139 °C illustrates 66.6% weight loss which is related to the decomposition of chemical compounds. Increasing temperature from 139 to 300 °C caused an 8% weight loss which can be attributed to the decomposition of more stable chemical components. According to the results obtained from the TGA test, it is concluded that the extracted natural surfactant is stable under the thermal conditions of the reservoir.

The FTIR transmittance spectrum of the CP was obtained in the range of 400−4000 cm^{-1}. Figure 3b illustrates the FTIR test results for CP. The hydroxyl group (O−H) and carbon-hydrogen (-CH2) absorbance are observed at 3416.39 cm^{-1} and 2084.89 cm^{-1}, respectively. A sharp peak at 1639.36 cm^{-1} indicates the existence of the amide group (C═O). Another peak at 1064.2 cm^{-1} is attributed to glycosidic linkage (C−O−C), and the C═C is observed at 712.92 cm^{-1}. According to the compounds approved in this FTIR test and compared to

https://doi.org/10.1021/acsomega.1c07182
ACS Omega 2022, 7, 24951−24972

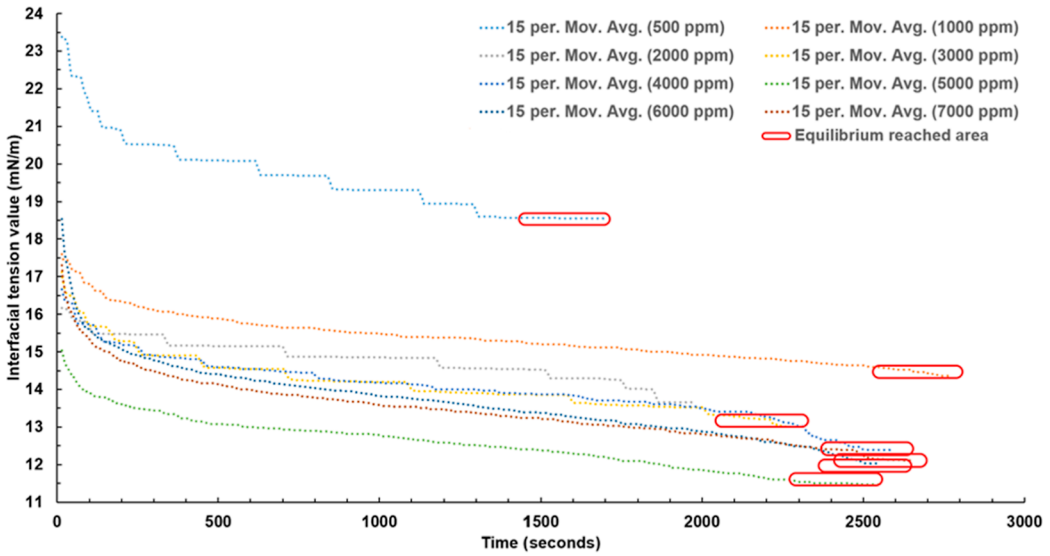

Figure 6. Dynamic measured IFT values of CP at different concentrations in DDW (different surfactant solutions) with crude oil under ambient temperature and pressure conditions.

the pure saponin spectrum, it is confirmed that the extracted solution contains saponin.[40−42]

3.2. Characterization of ZnO/MMT Nanocomposites. The FT-IR spectra of ZnO/MMT nanocomposites are shown in Figure 4a. The 3627.61 and 3698.09 cm^{-1} peaks correspond to the hydroxyl group (O−H). The bands at 3401.91 and 1639.66 cm^{-1} represent stretching and bending vibration of water, respectively. The sharp peak at 1036.39 cm^{-1} has been resulted in Si−O−Si groups of the tetrahedral sheets of MMT. The peaks at 793.46, 536, and 467.73 cm^{-1} represent the bending and stretching vibration of the Zn−O−Zn.[43−45] Based on the results obtained from the FTIR test applied to the synthesized nanocomposite, the correctness of the synthesis and the presence of ZnO and MMT compounds are confirmed.

Figure 4b presents the XRD spectra of the synthesized ZnO/MMT nanocomposite. Xpert High Score Plus software was used to analyze the results of the XRD test. Figure S5 shows the identified compounds of the synthesized nanocomposite. The XRD diffraction patterns show that the synthesized nanocomposite contains SiO_2, Fe_3O_4, ZnO, and MMT nanoparticles by peaks at 2θ values of 20.143, 21.13, 23.85, 25.32, 26.91, 27.983, 29.9, 35.34, 36.75, 42.7, 46, 50.392, 55.26, 60.223, 61.18, 68.3, and 73.65.

The morphology of the ZnO/MMT nanocomposite by the FE-SEM technique is illustrated in Figure 4c. Figure 4c shows the size, shape, homogeneity, and morphology of the synthesized nanocomposite at 500 nm-100kx and 200 nm-200kx magnification. According to the FE-SEM pictures, the size range of the synthesized nanocomposite is between 25 and 50. Therefore, the nanoscaled sizes of the synthesized green nanocomposite are confirmed.

3.3. Solution Properties. Figure 5 illustrates the electrical conductivity, pH, and density values of solutions at different concentrations. Column a corresponds to the CP solution, and column b corresponds to the nanofluid and hybrid solutions. Measurements of electrical conductivity and pH are common methods of obtaining the CMC point.[46,47] From Figure 5a, it can be seen that with increasing CP concentration, the electrical conductivity of the solution increases. It should be noted that from the concentration of 5000 ppm onward, the slope of the graph decreases and is not as sharp as the lower concentrations. Due to the change in the slope of the graph at 5000 ppm, this concentration is considered as the CMC point. Another method for obtaining the CMC is calculating the pH at different concentrations. In this research, by calculating the pH of different concentrations of the CP solutions, the CMC was obtained, and the result is presented in Figure 5a. From 500 to 5000 ppm, the pH value has a downward trend, but at concentrations above 5000 ppm, an upward trend is observed. According to the pH values and trend change at this point, like the electrical conductivity results, it is concluded that the CMC point is 5000 ppm. Figure 5 also shows the density values of the surfactant at different concentrations. It is clear that the density increases with increasing the CP concentration. Figure 5b illustrates the fluid properties of nanocomposites and hybrid solutions. From the electrical conductivity data of the nanocomposite shown in Figure 5b, it is clear that the conductivity has increased from 250 ppm, which is due to the release of ZnO electrons. It is also known that the conductivity of a hybrid solution is higher than that of a solution without a surfactant. In justification of the increase in electrical conductivity by the use of the CP extract, it could be mentioned that the CP extract includes different saponins that are categorized as nonionic surface-active agents, and also, an electric field of sufficient strength can generate electric conductivity. This phenomenon as explained by Onsager could be described by the break-up of "ion pairs" into separate free ions at high field strength.[48]

From the pH values of the nanocomposite and hybrid solutions in Figure 5b, it can be seen that the pH increases with increasing the concentration of the nanocomposite. The presence of different acidic components in the CP extracted reduces the pH in the hybrid solution compared to the nanofluid without the CP. The pH of the aqueous solution of the CP extract could be placed within 5.55 to 5.85 ranges that could act as a pH-reducing material. In hybrid solutions, the available materials within the extract could induce this property to the hybrid colloidal nanofluid and to the nanosized particles and decrease the total pH to a lower value if compared with

https://doi.org/10.1021/acsomega.1c07182
ACS Omega 2022, 7, 24951−24972

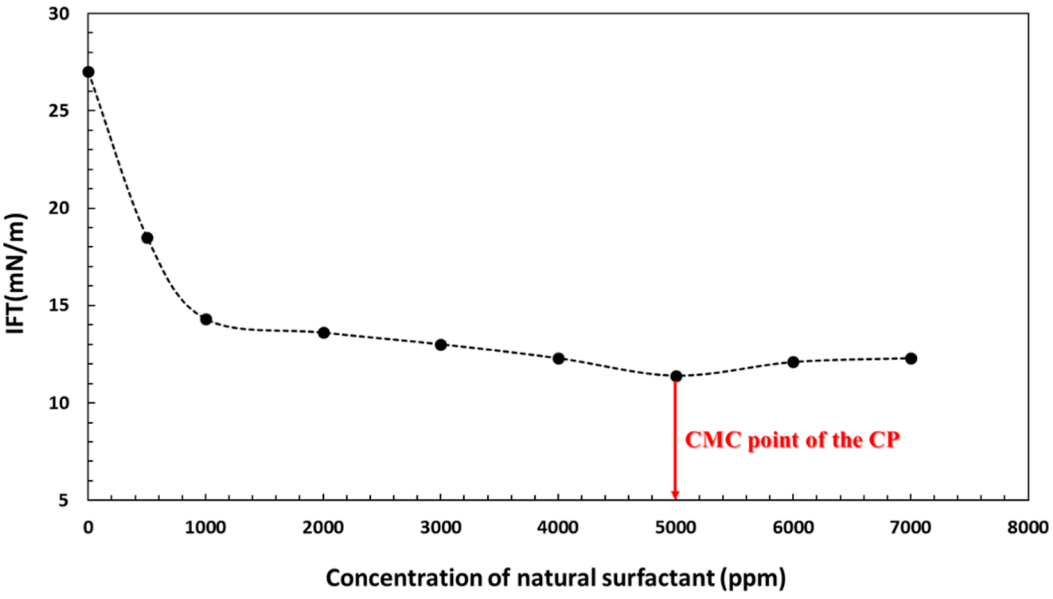

Figure 7. IFT values between water and oil in the presence of different concentrations of CP.

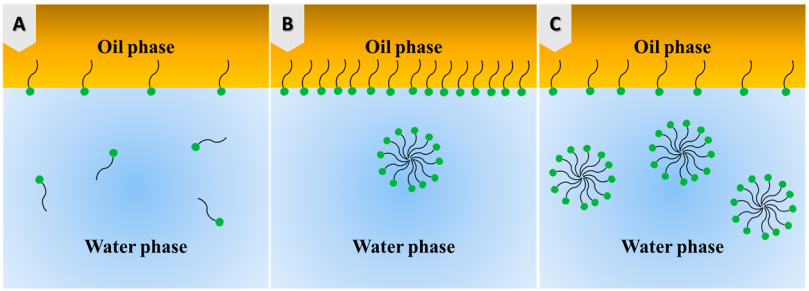

Figure 8. Mechanism of IFT alteration at various concentrations of the surfactant: (A) Below CMC. (B) At CMC. (C) Above CMC.

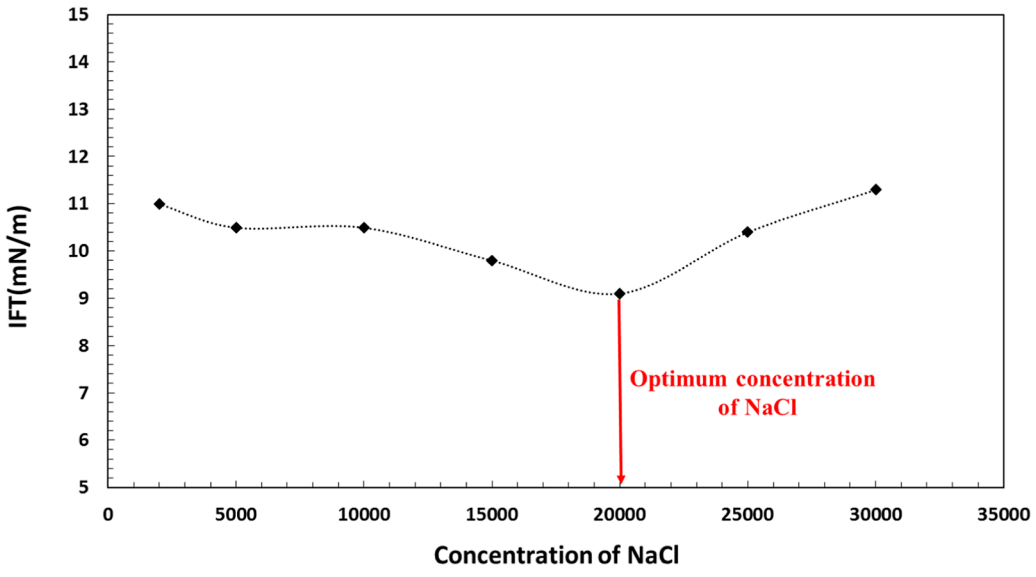

Figure 9. IFT values between water and oil in the presence of CP at CMC and different concentrations of NaCl.

approximate pH neutral colloidal nanofluids. The density data in Figure 5b show that the increase in ZnO/MMT concentration of the hybrid and nanocomposite solution increases the density.

3.4. IFT and Wettability Tests. *3.4.1. Natural Surfactant.* Various concentrations of the surfactant were applied to calculate the IFT between crude oil and DDW. CP concentrations of 500 to 7000 ppm were used to measure the IFT under ambient conditions. Figure 6 illustrates the dynamic IFT between the various concentrations of CP and crude oil. The vertical axis is the instantaneous measured IFT value reported through the applied software, and the dotted-

https://doi.org/10.1021/acsomega.1c07182
ACS Omega 2022, 7, 24951−24972

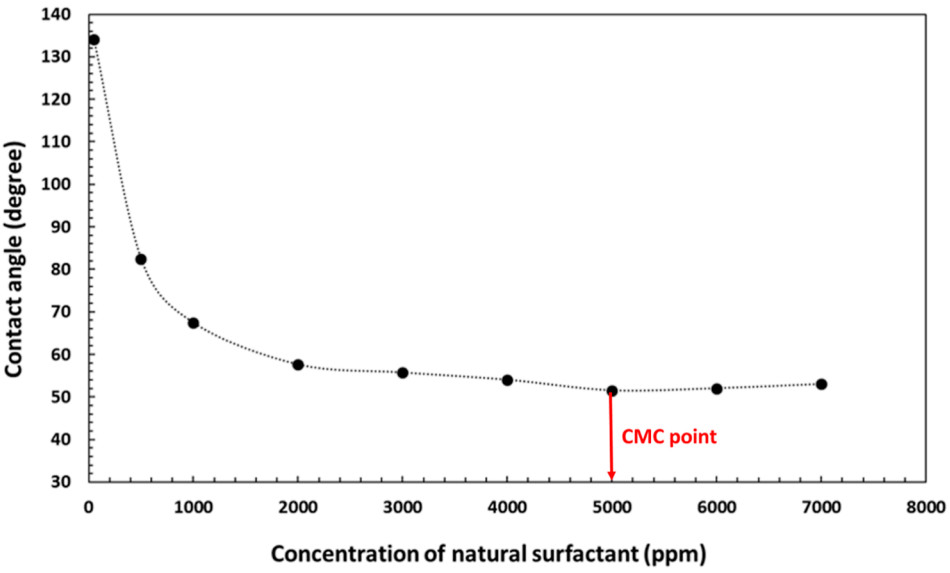

Figure 10. Contact angle values of the oil droplets on the surface of the carbonate pellets in the presence of different concentrations of CP.

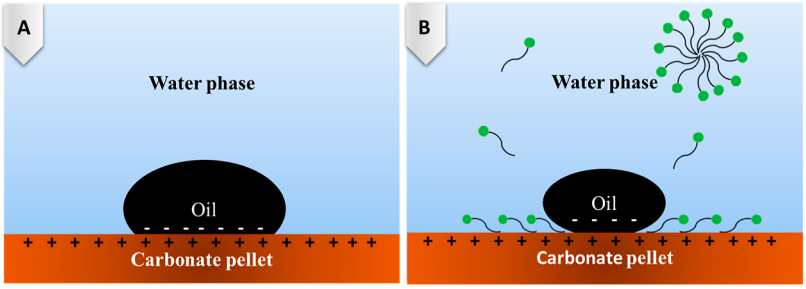

Figure 11. Mechanism of wettability alteration of an oil-wet carbonate rock in the presence of a nonionic surfactant. (A) Attach the oil droplet to oil-wet carbonate rock. (B) Wettability alteration of carbonate rock by the natural surfactant.

colored series are the 15 pointed moving averaged governed trend lines of the oscillating real IFT curves. Figure 7 shows the equilibrium values of the IFTs. The initial IFT value of DDW/crude oil was 27 mN/m, which decreased to 18.5, 14.3, 13.59, 13, 12.3, 11.4, 12.1, and 12.3 mN/m at 500, 1000, 2000, 3000, 4000, 5000, 6000, and 7000 ppm, respectively. As can be seen in Figure 7, the IFT decreases with increasing CP concentration up to 5000 ppm. The CMC point was detected at 5000 ppm, which indicates an 87.5% decrease. The CMC obtained from IFT measurements is consistent with the CMC obtained from the electrical conductivity and pH results. At concentrations above 5000 ppm, the IFT did not decrease.

CP as a surfactant tends to occupy the interface between two immiscible fluids, which alters the physical and chemical properties of the interface. The arrangement of the surfactant in a solution is such that the hydrophilic head is in the lipid part and the hydrophobic tail is in the water phase. Such a placement of surfactants reduces the IFT between the two immiscible fluids. The optimal concentration of the surfactant to reduce IFT is the micelle formation concentration. At higher concentrations of CMC, the IFT increases because more surfactants participate in the formation of micelles, and their numbers decrease at the oil–water interface (Figure 8).[49]

After identifying the CMC point of the CP, IFT values at 2000, 5000, 10 000, 15 000, 20 000, 25 000, and 30 000 ppm concentrations of NaCl were investigated at the CMC point of CP. As can be seen in Figure 9, the CP surfactant shows better performance in the presence of NaCl. The NaCl reduces the IFT value of crude oil/DDW from 11.4 to 9.1 mN/m at the 20 000 ppm concentration of NaCl as the optimum concentration.

When the ions of salts are joined into reactions, the variation of IFT values could be affected by the positioning of ions at the interface and adsorption of ions on this intermediate phase boundary: The origination of positioning of ions from aqueous solution at the interface in the positioning of oil polar components such as available asphaltenes at the interface from the other phase. At low concentrations, the salt-in effect occurs and causes a decrease in IFT at this interface. In this state, the organic particles tend to be dissolved in the aqueous solution, while in pure water, the aquatic molecules create a strong structure on one side of the water–organic matter interface and do not allow any disorder in their interfacial arranged structure and any entrance of organic molecules to the water phase. Therefore, any interface disturbance is low, and reduction of the IFT value is not achieved. In a low saline solution, positively charged sodium ions surround the oil droplet due to negative charges and adhere to it. This phenomenon causes the water molecules to adhere to the oil droplet. This behavior causes an IFT reduction between water and oil up to a certain salt concentration, and after that, the IFT increases. The reason for this increase is that with the increase in salt concentration, sodium ions in the environment

https://doi.org/10.1021/acsomega.1c07182
ACS Omega 2022, 7, 24951−24972

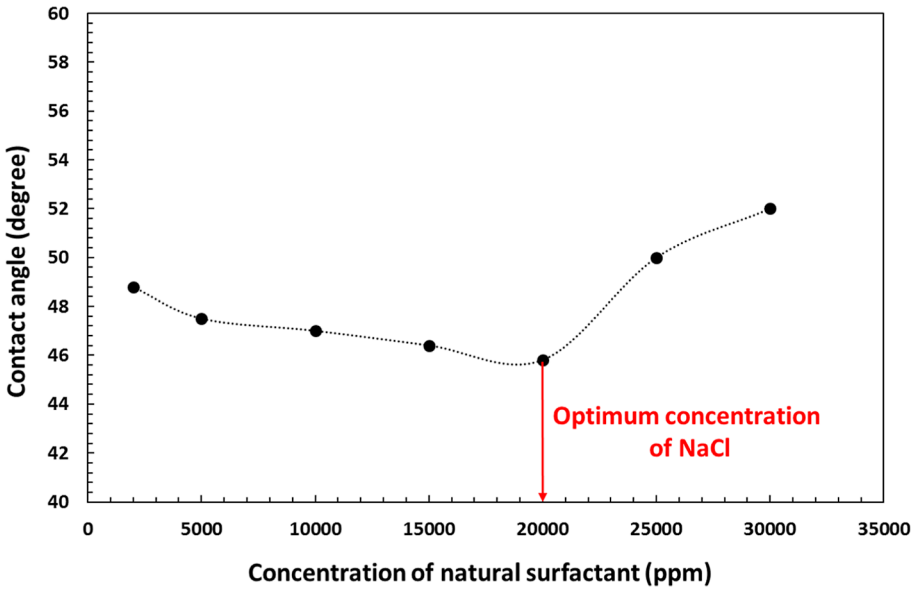

Figure 12. Contact angle values of the oil droplets on the surface of the carbonate pellets in the presence of CP at CMC and different concentrations of NaCl.

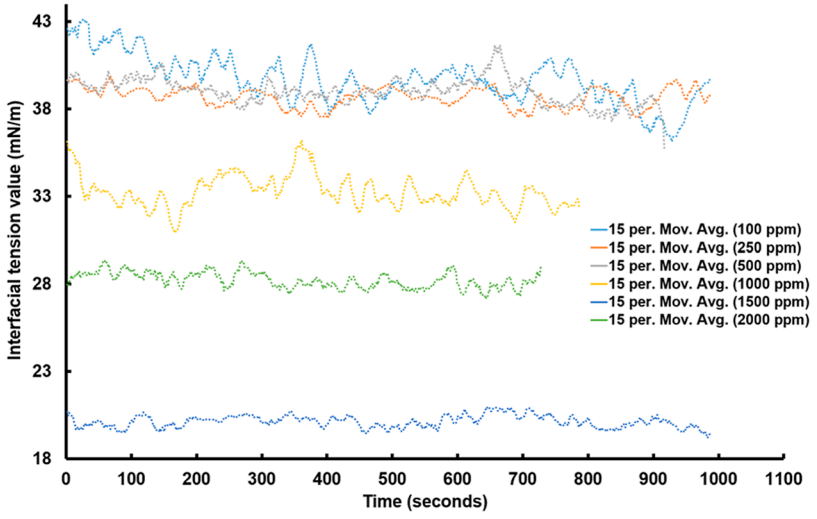

Figure 13. Measured dynamic IFT values at different concentrations of the synthesized nanocomposite in DDW (different nanofluid concentrations) with crude oil under ambient conditions.

increase and water molecules become involved in sodium ions in the environment and fewer water molecules attach to oil.[50]

In this study, the contact angle method was used to study the wettability alteration of carbonate rock. Figure 10 shows the changes in the contact angle of oil droplets on the carbonate rock surface versus different concentrations of CP under ambient conditions. The initial value of the contact angle of the oil drop on the oil-wet carbonate surface was 134°, which decreased to 82.5, 67.4, 57.6, 55.7, 54, 51.5, 52, and 53° at 500, 1000, 2000, 3000, 4000, 5000, 6000, and 7000 ppm of CP, respectively. The trend of contact angles has been decreased from 0 to 5000 ppm and then increased, and the lowest value of the contact angle was obtained at a concentration of 5000 ppm, which was identified as the CMC point.

The reason for the oil droplets sticking to the surface of the carbonate rock is the negative charge of oil composition such as stearic acid ($R\text{-}COO^-$), which is adsorbed by the positive charge ($-Ca^+$) of the carbonate rock, and this is an electrostatic interaction.[51] CP as a nonionic surfactant contains benzene rings in its hydrophobic tail, which are the source of electrons. The tail of the saponin adheres onto the positive surface of the carbonate rock and forms a thin layer that alters the wettability from oil-wet to water-wet.[52] Figure 11 shows the wettability alteration mechanism by a nonionic surfactant.

After determining the CMC point of CP from the contact angle measurements, the wettability alteration of carbonate rock was performed in the presence of different concentrations of NaCl and CMC of the surfactant as the base solution. 2000, 5000, 10000, 15 000, 20 000, 25 000, and 30 000 ppm of NaCl were added to the CMC solution of CP, and the wettability alteration of carbonate rock at these concentrations was investigated. As can be seen in Figure 12, NaCl shows a synergy effect with CP to reduce the contact angle. From 2000 to 20 000 ppm of NaCl, the contact angle trend was decreasing, but at concentrations above 20000 ppm, the

https://doi.org/10.1021/acsomega.1c07182
ACS Omega 2022, 7, 24951−24972

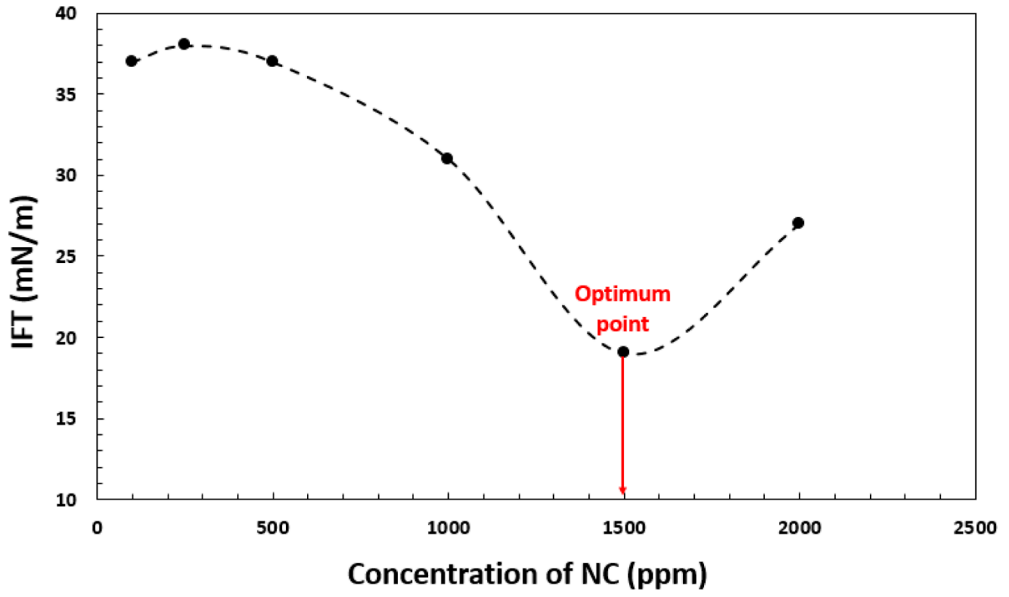

Figure 14. IFT value between water and oil in the presence of nanocomposite solutions.

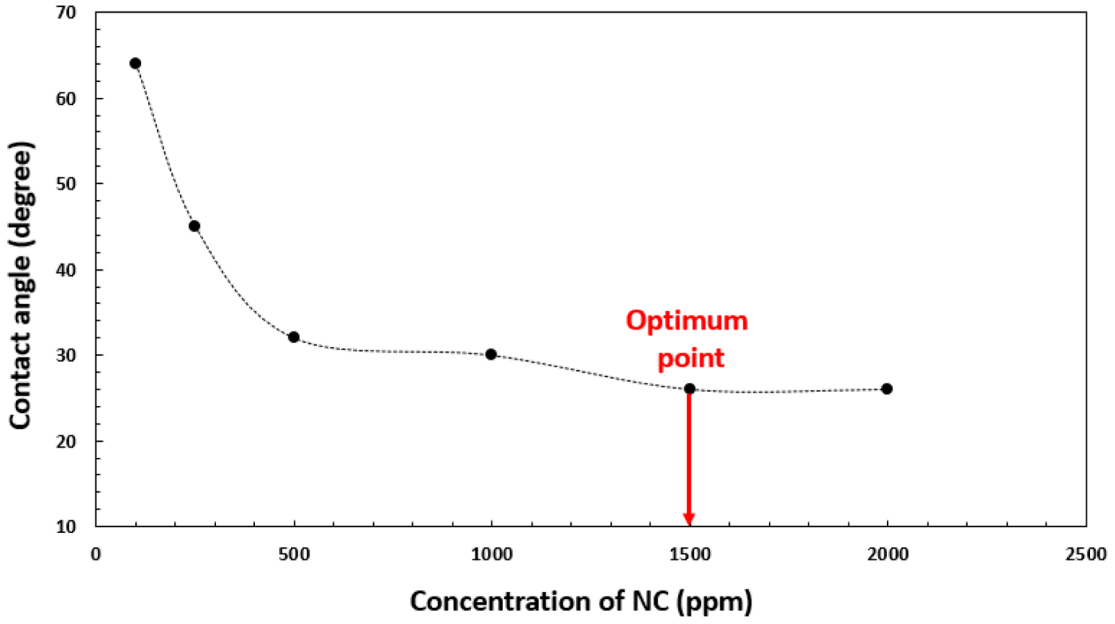

Figure 15. Contact angle of oil droplets to the carbonate pellets in the presence of nanocomposite solutions.

contact angle trend was increasing. As a result, 20 000 ppm of NaCl was identified as the optimal concentration, which represents 60% optimization compared to the initial value. The same procedure of the salting-in effect like its impact on IFT change applies here in alteration of the wettability state. This salinity effect causes a reduction release of active polar components adhered previously to the rock surface. Sodium ions allow oil droplets to easily separate from the rock surface. For this reason, the surface wettability of carbonate rock in the surfactant and salt solution is more hydrophilic than surfactant solution and DDW solution.

3.4.2. Nanocomposite Solution (ZnO/MMT). IFT experiments were conducted at different concentrations of the synthesized ZnO/MMT nanocomposite under the ambient condition. Figure 13 shows the dynamic IFT values of different concentrations of nanocomposite solutions during the time. The vertical axis is the instantaneous measured IFT value reported through the applied software, and the dotted-colored series are the 15 pointed moving averaged governed trend lines of the oscillating real IFT curves. Figure 14 illustrates the IFT values of the nanocomposite solutions as the equilibrium IFT values, which were obtained from the dynamic IFT measurements. As shown in this figure, ZnO/MMT nanocomposites initially increases the IFT at a concentration of 100 to 250, but after increasing the concentration, the IFT decreases. There was an abnormality for the nanofluid at a concentration of 250 ppm of nanocomposites for both electrical conductivity and IFT measurements. At concentrations of 100 and 250 ppm of the nanocomposite, MMT reduces the electrical conductivity of the solution. At higher concentrations than 250 ppm, the concentration of ZnO increases, and the conductivity of

https://doi.org/10.1021/acsomega.1c07182
ACS Omega 2022, 7, 24951−24972

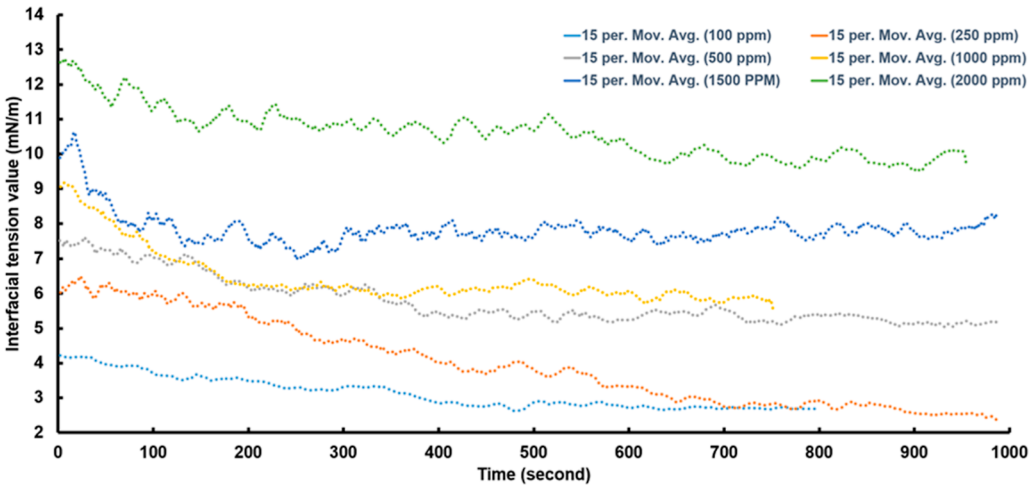

Figure 16. Measured dynamic IFT values of different concentrations of the synthesized nanocomposite in CMC solutions of the surfactant (different hybrid concentrations).

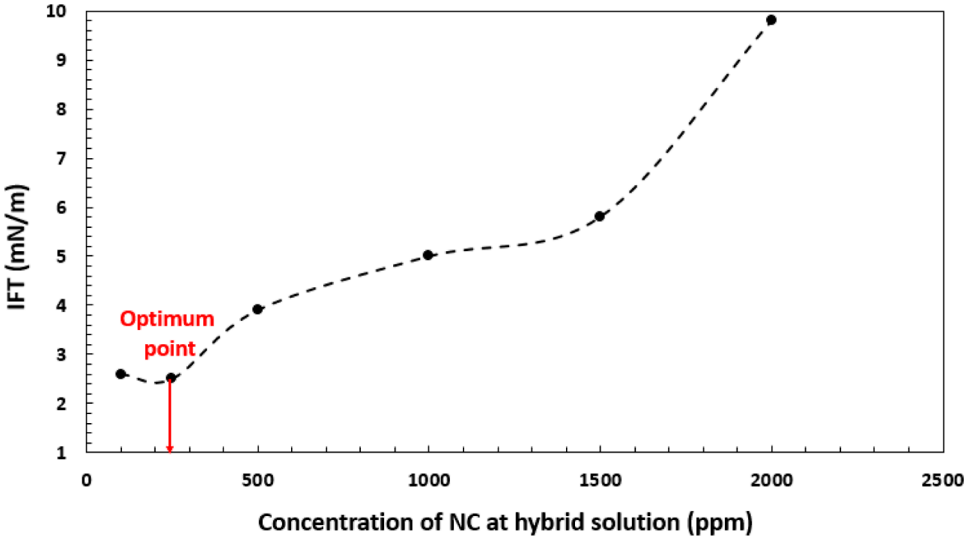

Figure 17. IFT values between water and oil in the presence of the CP−ZnO/MMT hybrid solutions vs different concentrations of ZnO/MMT nanocomposites.

nanocomposites also increases due to the generation of free electrons.[53]

At the selected concentration of 1500 ppm, the lowest IFT 19 mN/m was obtained and considered as the optimum concentration. Although this nanocomposite was not very successful in reducing the IFT, the main purpose of the nanocomposites is not to reduce IFT. Therefore, other mechanisms such as wettability alteration should be investigated.

Wettability alteration is one of the most important effective parameters of nanofluids in increasing the oil recovery from the reservoirs. Hence, the contact angle measurements were conducted in the presence of different concentrations of ZnO/MMT under ambient conditions.

Figure 15 shows the contact angle values of the oil droplets with carbonate pellets at different concentrations of the nanofluid. According to the contact angle measurement results, the ZnO/MMT nanocomposite was able to alter the wettability of the carbonate rock from oil-wet to water-wet. As can be seen from Figure 15, until 1500 ppm, with increasing concentration of NC, the contact angles have decreased. The concentrations of 100, 250, 500, 1000, 1500, and 2000 ppm result in contact angles of 63.94, 45, 32, 30, 26, and 26°, respectively. Although higher concentrations of nanofluids are usually more effective in altering wettability, they may reduce the permeability of the reservoir rock.[54]

The concepts of nanofluids and resulting wettability alteration should be discussed in a procedure that causes nanofluids to affect the surface wettability of rocks. Nanofluids are fluids that include dispersed nanoparticles with a diameter of 1−100 nm.[55,56] Nanofluids generate a thin film on the surface of the solid, according to Chengara, Nikolov, Wasan, Trokhymchuk, and Henderson (2004), and the consequent restrictions of the positioning of the nanomaterials inside of this film force the nanomaterials to emerge in regular layers.[57] The entropy of the whole system grows as a result of the increased space available for the nanomaterials' twisted movement, and as a result, a tremendous pressure value is induced on the system's restricted volume. The configuration and size of nanoparticles can affect the generated pressure profile.[58] According to McElfresh, Olguin, Ector, and others (2012), a thin film diffused over the rock's surface can separate

https://doi.org/10.1021/acsomega.1c07182
ACS Omega 2022, 7, 24951−24972

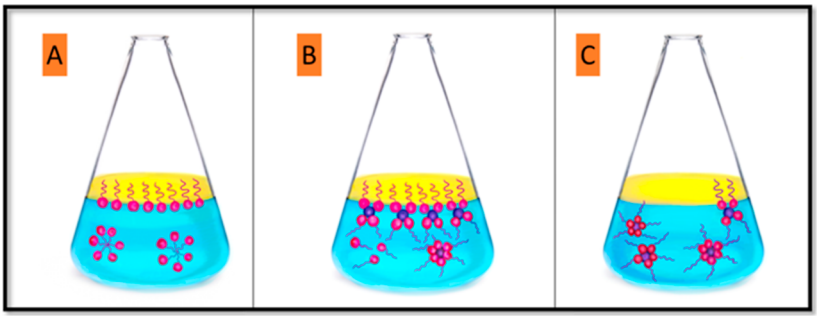

Figure 18. Mechanism of a hybrid solution to change IFT: (A) surfactant solution at CMC concentration. (B) Hybrid solution at the optimum concentration of nanocomposites. (C) Decreasing nanosurfactants at the interface of oil−water by increasing the nanocomposite concentration.

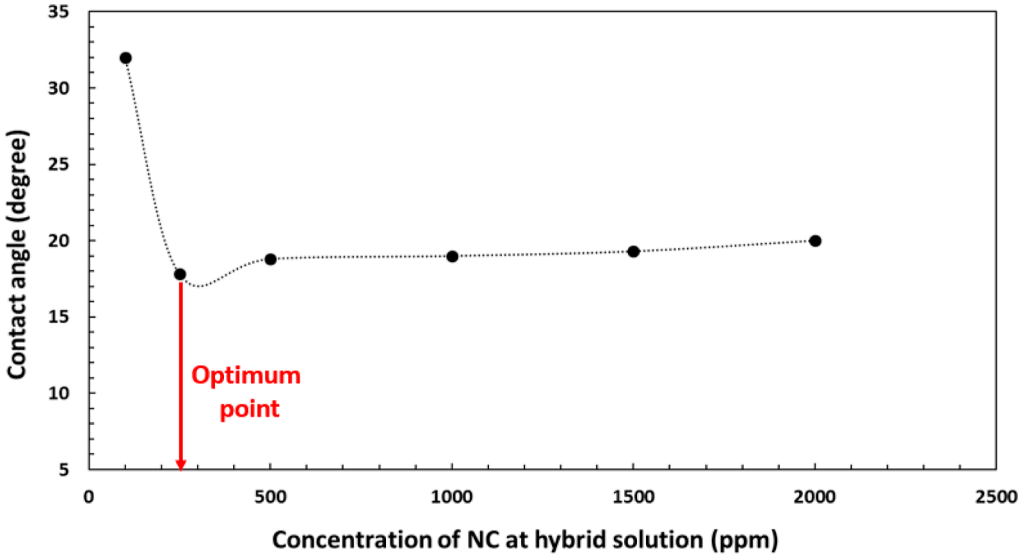

Figure 19. Contact angle values of the oil droplets on the surface of the carbonate pellets in the presence of hybrid solutions versus different concentrations of the nanocomposite.

adherent oil, paraffin, and gas from the rock surface.[59] The separation of these components, which causes the rock to be oil-wetting, ends in a water-wetting situation. When compared to the fluid and reservoir rock, the intensity of this phenomenon is mostly determined by the characteristics of the nanofluid and dispersed nanoparticles. The effects of altering the wettability of nanosized materials lead the film to form. The development of pressure in the system also results in the formation of a wedge-like film, which is referred to as structural disjoint pressure.[59] It is caused by Brownian motion (random movements of suspended nanoparticles in a fluid) and repulsive electrostatic interactions between nanoparticles.[60,61] According to Aveyard, Binks, and Clint, the properties of the rock surface, the temperature of the base fluid, salt content, and, in particular, the quantity and size of nanoparticles all impact the nanofilm's progression. An elevated level of nanoparticle particle numbers leads to an amplification of disjoint overpressure in the system and a consequent decrease in the contact angle if no other mechanism—such as the attraction of nanocomposites on the surface of solid rock—disputes with the nanofilm. Increasing concentrations leads to larger disjointed pressure values, resulting in a reduction of contact angle values.[62]

3.4.3. Hybrid Solution (CP−ZnO/MMT). In this step, the IFT between oil and different concentrations of ZnO/MMT as a solute in the hybrid solution was measured. To make the hybrid solution, the CP at the CMC which was obtained earlier from electrical conductivity, pH, IFT, and contact angle methods was used as the dispersing agent, and the ZnO/MMT nanocomposite with different concentrations was used as the dispersed agent. 100, 250, 500, 1000, 1500, and 2000 ppm of ZnO/MMT nanocomposites were used to make hybrid solutions and then used in the IFT and contact angle measurements. Figure 16 illustrates the dynamic IFTs in the presence of different concentrations of nanocomposites in the hybrid solution. The vertical axis is the instantaneous measured IFT value reported through the applied software, and the dotted-colored series are the 15 pointed moving averaged governed trend lines of the oscillating real IFT curves. Figure 17 presents the equilibrium values of the IFTs in the presence of different concentrations of the nanocomposite. 2.6, 2.4, 5, 5.8, 7.7, and 9.8 mN/m were obtained at concentrations of 100, 250, 500, 1000, 1500, and 2000 ppm of nanocomposites in the hybrid solution, respectively. Compared to the CP, the hybrid solution significantly reduces the IFT. The optimal concentration of the nanocomposite at the hybrid solution was observed at 250 ppm which shows an 80% reduction in IFT. The reason for this significant reduction in IFT is due to the stability created in the new solution (Figure 18B). At concentrations higher than 250 ppm, the IFT increases because the surfactants become more involved with the

https://doi.org/10.1021/acsomega.1c07182
ACS Omega 2022, 7, 24951−24972

Table 1. Results of IFT and Contact Angle Measurements in the Presence of Different Solutions

material	concentration (ppm)	IFT (mN/m)	contact angle (θ)	base solution
CP (surfactant)	0	27	134	DDW
	500	18.5	82.5	
	1000	14.3	67.4	
	2000	13.59	57.6	
	3000	13	55.7	
	4000	12.3	54	
	5000	**11.4**	**51.5**	
	6000	12.1	52	
	7000	12.3	53	
CP + NaCl	CMC+ 0	11.4	51.5	CMC of surfactant (5000 ppm of CP)
	CMC+2000	11	48.8	
	CMC+5000	10.5	47.5	
	CMC+10 000	10.5	47	
	CMC+15 000	9.8	46.4	
	CMC + 20 000	**9.1**	**45.8**	
	CMC + 25 000	10.4	50	
	CMC + 30 000	11.3	52	
ZnO/MMT (nanocomposite)	0	27	134	DDW
	100	37	63.94	
	250	38	45	
	500	37	32	
	1000	31	30	
	1500	**19**	**26**	
	2000	27	26	
CP + ZnO/MMT (hybrid)	CMC + 0	11.4	51.5	CMC of surfactant (5000 ppm of CP)
	CMC + 100	2.6	32	
	CMC + 250	**2.4**	**17.8**	
	CMC + 500	5	18.8	
	CMC + 1000	5.8	19	
	CMC + 1500	7.7	19.3	
	CMC + 2000	9.8	20	

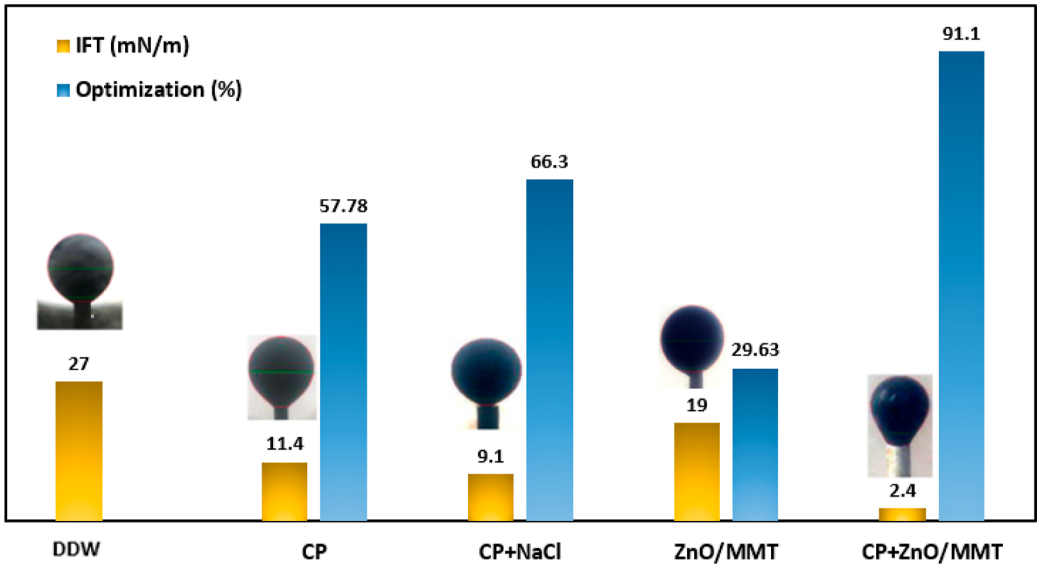

Figure 20. Optimization percentages of IFT measurements in the presence of different solutions.

nanocomposite, and their amount at the oil–water interface decreases (Figure 18C).

Figure 19 illustrates the results of contact angle measurements of CP-ZnO/MMT solutions which were measured at concentrations of 100 to 2000 ppm of ZnO/MMT nanocomposites. As the results show, 32, 17.82, 18.8, 19, 19.3, and 20° were obtained at concentrations of 100, 250, 500, 1000, 1500, and 2000 ppm of the nanocomposite, respectively. The lowest contact angle was obtained at 250 ppm which reduced the contact angle from the initial value of 134 to 17.82° which shows 86.7% optimization. This hybrid fluid has altered the wettability from oil-wet to strong water-wet.

https://doi.org/10.1021/acsomega.1c07182
ACS Omega 2022, 7, 24951−24972

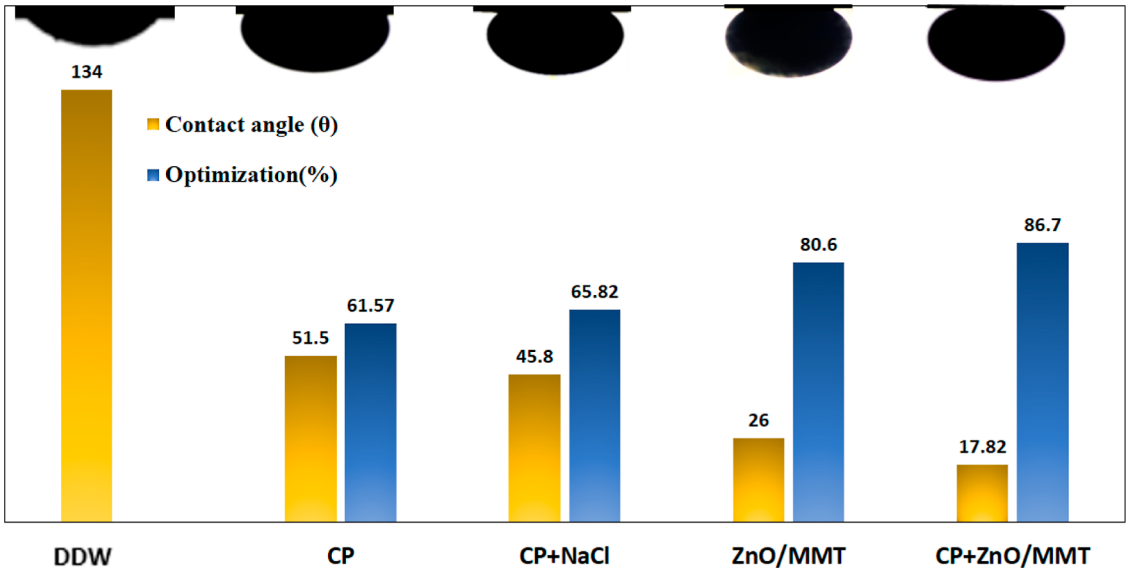

Figure 21. Optimization percentages of wettability alteration tests in the presence of different solutions.

Table 2. Specifications of Carbonate Cores

core number	diameter (cm)	length (cm)	bulk volume (cm^3)	dry core weight (gr)	saturated core weight (gr)	PV (cm^3)	porosity (%)	permeability (MD)	S_{wirr} (%)	OOIP (%)
no. 1	3.74	6.5	71.37	164.35	178	8.4	11.76	3.5	36.54	63.46
no. 2	3.74	6.79	74.55	178.038	187.038	9.612	12.89	3.6	38.4	61.6
no. 3	3.74	5.65	62.04	148.8	155.3	6.5	10.48	3.9	38.46	61.54

3.5. Comparison of IFT and Wettability Alteration Test Results. All the results of the IFT and wettability alteration tests in the presence of CP, CP + NaCl, ZnO/MMT, and CP + ZnO/MMT as hybrid solutions are reported in Table 1. As mentioned in the previous sections, all of the tests were performed under ambient conditions. According to the results obtained from IFT measurements in different solutions, it has been observed that the CP is able to reduce the IFT from the initial value of 27 to 11.4 mN/m at 5000 ppm as CMC. Also, by adding NaCl to the CMC of CP, its performance is improved and the IFT is reduced to 9.1 mN/m at 20 000 ppm of NaCl. The nanofluid increases the IFT between oil and water at low concentrations. At 1500 ppm of the nanocomposite as the optimum concentration of the ZnO/MMT nanofluid, the IFT decreases from an initial value of 27 to 19 mN/m, which indicates 29% optimization. By measuring the IFT of oil−water in the presence of the hybrid solution of CP and ZnO/MMT, 2.4 mN/m is obtained as the optimum value at 250 ppm of the ZnO/MMT nanocomposite. In other words, the obtained optimization percentages for CP, CP + NaCl, and the CP + ZnO/MMT nanofluid are 57.78, 66.3, and 91.1%, respectively (Figure 20).

The wettability alteration of carbonate rocks in the presence of different solutions was investigated, and the results at the optimal concentration for each solution are presented in Figure 21. At the CMC of CP, the contact angle decreases from 134 to 51.5°. In other words, this surfactant alters the wettability from oil-wet to water-wet. By adding NaCl to the surfactant, the contact angle is reduced more until a contact angle value of 45.8° is obtained at 20000 ppm of NaCl and the CMC of the surfactant. Then, the wettability alteration of carbonate rock in the presence of the ZnO/MMT nanocomposite was studied. The ZnO/MMT nanocomposite is able to alter the wettability from oil-wet to water-wet. At an optimum concentration of 1500 ppm of ZnO/MMT, the contact angle decreases from the initial value of 134° to 26°. The best results of wettability alteration tests were obtained in the presence of the nanocomposite-surfactant hybrid solution. In other words, the hybrid solution is able to reduce the contact angle of the oil droplet to 17.82°, which indicates strong water-wet wettability. As can be seen in Figure 21, the optimization percentages for CP, CP + NaCl, ZnO/MMT nanofluid, and hybrid solutions to wettability alteration are 61.57, 65.82, 80.59, and 86.70%, respectively.

3.6. Core Flooding and Reservoir Properties. To evaluate the potential of the natural surfactant, nanocomposite, and hybrid solutions, three flooding experiments at the optimum concentrations of CP + NaCl (CMC + 20 000 ppm of NaCl), nanocomposite (1500 ppm), and hybrid (CMC + 250 ppm of nanocomposite) solutions under ambient conditions were performed. In this study, three carbonate cores were used to perform core flooding tests. The specifications of each core can be seen in Table 2. First, the cores were saturated with seawater, and the saturated core weight was measured. By subtracting the saturated weight from the dry weight of the core, the PV of each core was obtained. Also, by dividing the obtained PVs by the density of seawater, the volume of water in the cores was obtained. In the next step, oil was injected into the cores until no more water was produced from the cores. By reducing the volume of produced water from the total amount of water in the pores, the irreducible water of each core was obtained. As can be seen in tale 4, the irreducible water was 36.54, 38.4, and 38.46% for cores number 1, 2, and 3, respectively.

After saturating the cores with crude oil and achieving irreducible water saturation, seawater was injected into the

https://doi.org/10.1021/acsomega.1c07182
ACS Omega 2022, 7, 24951−24972

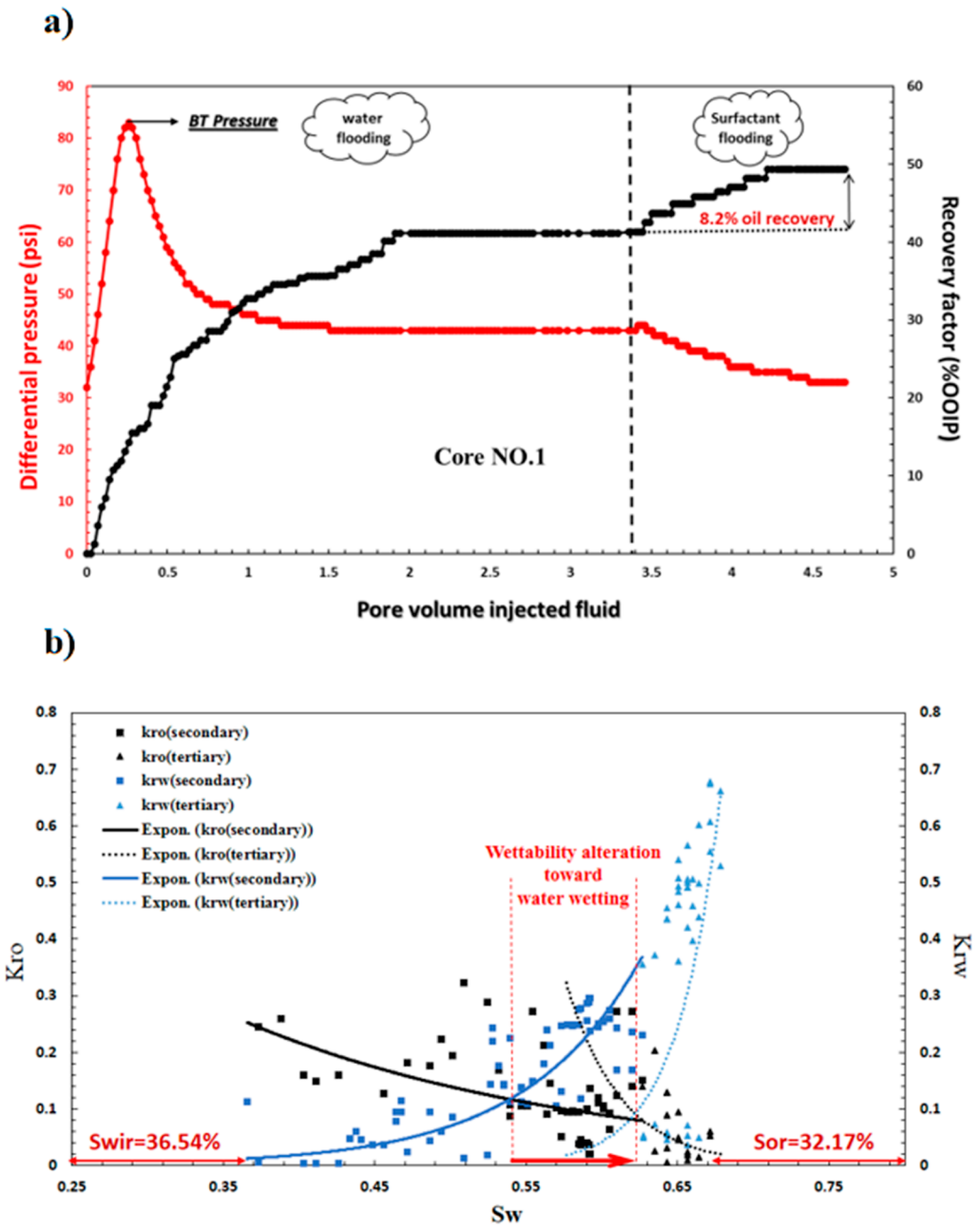

Figure 22. Dynamic core flooding results: (a) oil recovery by water and CP flooding and (b) relative permeability curve of water and the surfactant by the JBN method.

cores at 0.2 cm^3/min rates to produce oil from the cores as secondary production. The oil recovery, pressure, and PV of injection into cores 1, 2, and 3 are illustrated in Figures 22, 23, and 24, respectively. The secondary production is 41.12, 43.16, and 42.5% for core nos. 1, 2, and 3, respectively. Also, according to the pressure diagram, the breakthrough points for core nos. 1, 2, and 3 occur at 0.28, 0.27, and 0.24 PV, respectively.

CMC of CP solution (5000 ppm) at the optimum concentration of NaCl (20000 ppm) was injected into the core no. 1 to investigate the effect of the natural surfactant on increasing oil recovery. Figure 22 illustrates the results of water and surfactant flooding. After 3.4 PV water flooding, the CP solution was injected into the core no. 1. As can be seen in Figure 22a, the flooding process at this step continued until 4.8 PV, in which the oil production was not increased more. By injecting surfactant solution after water flooding, the RF increased from 41.12 to 49.3%, which indicates an 8.2% additional oil recovery. Figure 22b shows the relative permeability curve of water and surfactant flooding by the JBN method.

To investigate the effect of nanocomposites on increasing oil recovery, a solution with a concentration of 1500 ppm of the ZnO/MMT nanocomposite was injected into core no. 2 as the secondary recovery step. As shown in the Figure 23a, the nanofluid has increased oil production from 43.16 to 49.2%. The nanocomposite has the ability of 6% additional oil recovery. Figure 23b presents the relative permeability curve of nanocomposite flooding obtained from the JBN method.

https://doi.org/10.1021/acsomega.1c07182
ACS Omega 2022, 7, 24951−24972

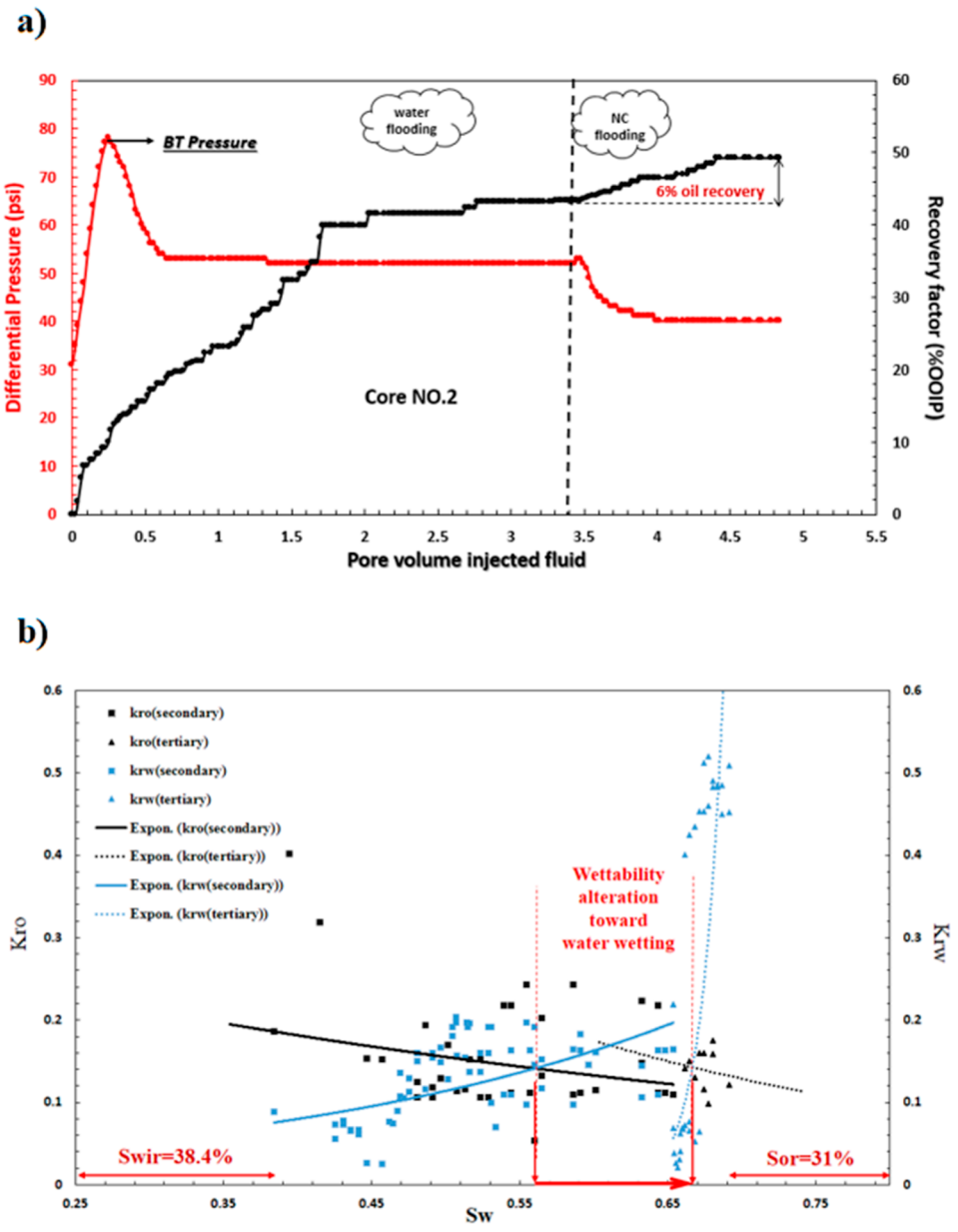

Figure 23. Dynamic core flooding results: (a) oil recovery by water and nanofluid flooding and (b) relative permeability curve of water and the nanofluid by the JBN method.

Adding nanocomposites to the surfactant as a hybrid agent can improve the performance of the surfactant, and the results obtained from the pendant drop and contact angle tests confirm this statement. According to the results obtained from the previous tests, the optimum concentration of the CP-ZnO/MMT nanocomposite solutions was identified at concentrations of 5000 ppm of CP as CMC and 250 ppm of the ZnO/MMT nanocomposite. Like the surfactant flooding, the nanofluid was injected into the core after the water flooding. The oil recovery was fixed after 4.6 PV injection. The oil recovery of water flooding of core no. 3 was 42.5% which increased to 55.5% after nanofluid flooding. In other words, 13% additional oil recovery was obtained by nanofluid flooding (Figure 24a). Figure 24b shows the relative permeability curve of water and nanocomposite-surfactant flooding by the JBN method.

The optimized values for contact angle modifications in CP + NaCl, ZnO/MMT, and CP + ZnO/MMT systems are 65.82, 80.6, and 86.7% in turn, while analysis of relative permeability curves shows different values for the same systems. By governing optimized values for analysis of the wettability alteration in carbonate and sandstone systems, intersection points could be analyzed and their shifts to higher water saturations are inferred as a more water-wet state. Therefore, by measurement of these intersection points, optimized values of 15.7, 19.64, and 4.6% are gained for CP + NaCl, ZnO/MMT, and CP + ZnO/MMT systems, respectively. These optimized values are different from each other for even the same systems because of the effects of different parameters in each system. In contact angle measurement experiments, all rock pellets were polished to eliminate the surface roughness effect, while in the porous medium, the parameter of surface roughness is included within the wettability shifting system. Another reason could be the lithological heterogeneities that are included in the porous medium, while their impacts were eliminated in contact angle measurement experiments. The

https://doi.org/10.1021/acsomega.1c07182
ACS Omega 2022, 7, 24951−24972

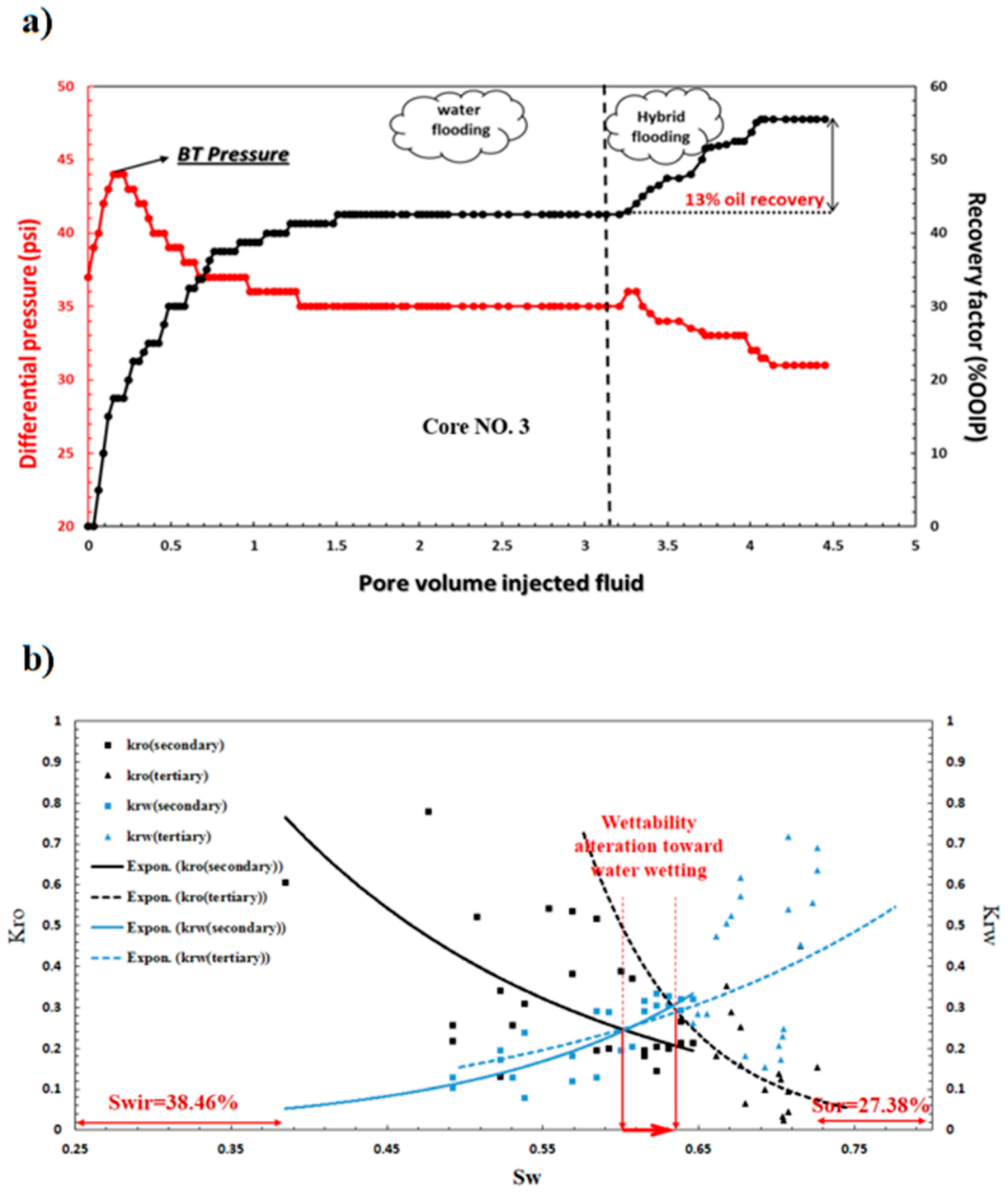

Figure 24. Dynamic core flooding results: (a) oil recovery by water and hybrid solution flooding and (b) relative permeability curve of water and hybrid solution by the JBN method.

time of fluid/solid contact is also different in contact angle measurement experiments and dynamic core flooding experiments that gain different results in this comparison. The observation of wettability alteration in each dynamic core flooding system is a difference of the wettability state induced by both seawater and EOR fluid, while in contact angle measurement experiments, EOR fluids were analyzed with the initial oil-wetted state.

The following equations were used to calculate the mobility ratio and capillary number[63,64]

$$M = \frac{(k/\mu)_{\text{water}}}{(k/\mu)\text{oil}}$$

where M, k, and μ are the mobility ratio, relative permeability, velocity, and viscosity, respectively.

$$C_a = \frac{\mu V}{\gamma}$$

where C_a is the capillary number, μ represents the viscosity, V stands for the velocity, and γ shows water−oil IFT.

https://doi.org/10.1021/acsomega.1c07182
ACS Omega 2022, 7, 24951−24972

According to the calculated relative permeability of oil and water for secondary water injection and viscosity values, mobility ratios of 27.64, 28.2, and 29.4 were obtained for core nos. 1, 2, and 3, respectively. Based on the IFT values of IFT of 27 mN/m during water flooding as secondary flooding, capillary numbers of 3.7×10^{-7}, 2.5×10^{-7}, and 2.8×10^{-7} were obtained for core nos. 1, 2, and 3, respectively. Like the secondary flooding step, the mobility ratio was calculated for tertiary steps, and the 10.65, 8.3, and 10.15 values were obtained for the surfactant, nanocomposite, and hybrid flooding, respectively. The capillary numbers 7.3×10^{-6}, 9.1×10^{-6}, and 6.7×10^{-6} were obtained for the surfactant, nanocomposite, and hybrid flooding, respectively.

4. CONCLUSIONS

CP plant was introduced as a new natural surfactant source, and the performance of the natural surfactant was investigated in the presence of the ZnO/MMT nanocomposite as a hybrid solution on the EOR. The following results were obtained:

(1) The IFT measurements show that the CP at CMC has the potential to reduce IFT of the oil−water from 27 to 11.4 mN/m. Also, by adding NaCl to the CMC of CP, this amount is reduced to 9.1 mN/m.
(2) Although the ZnO/MMT nanocomposite solution does not perform well in reducing the IFT between oil and water, in combination with the extracted surfactant as a hybrid agent, it is able to reduce the IFT well and reduce its value from 27 to 2.5 mN/m.
(3) The results of wettability alteration tests demonstrate that the CP surfactant alters the surface of carbonate rock to the weakly water-wet. When the various concentrations of NaCl are combined with the CP surfactant at CMC, the wettability becomes more water-wet.
(4) Nanofluids have a better performance than the extracted surfactant in altering the wettability, which alters the wettability from oil-wet to strong water-wet.
(5) Core flooding experiment results show 8.2, 6, and 13% additional oil recovery for the surfactant at optimum salinity, nanocomposite, and hybrid solution at the optimum concentrations of the nanocomposite, respectively.

■ ASSOCIATED CONTENT

Supporting Information

The Supporting Information is available free of charge at https://pubs.acs.org/doi/10.1021/acsomega.1c07182.

Summary of the effects of utilized natural surfactants in the field of EOR, summary of the effects of nano-surfactant solutions in the field of EOR, composition of the seawater, compositional properties of the used crude oil, structure of the CP extract, XRD of the carbonate rock sample, schematic of the used pendant and sessile drop apparatus designed by authors , schematic of the utilized core flood apparatus, and peak list of synthesized nanocomposites and identified compounds (PDF)

■ AUTHOR INFORMATION

Corresponding Authors

Abbas Khaksar Manshad − *Department of Petroleum Engineering, Abadan Faculty of Petroleum, Petroleum University of Technology (PUT), Abadan 6318714331, Iran*; Email: khaksar@put.ac.ir

Amir H. Mohammadi − *Discipline of Chemical Engineering, School of Engineering, University of KwaZulu-Natal, Durban 4041, South Africa*; orcid.org/0000-0002-2947-1135; Email: amir_h_mohammadi@yahoo.com

Authors

Ahmad Nourinia − *Department of Petroleum Engineering, Abadan Faculty of Petroleum, Petroleum University of Technology (PUT), Abadan 6318714331, Iran*

Seyed Reza Shadizadeh − *Department of Petroleum Engineering, Abadan Faculty of Petroleum, Petroleum University of Technology (PUT), Abadan 6318714331, Iran*

Jagar A. Ali − *Department of Petroleum Engineering, Faculty of Engineering, Soran University, Kurdistan Region 44008, Iraq*; orcid.org/0000-0002-7327-4243

Stefan Iglauer − *Discipline of Petroleum Engineering, School of Engineering, Edith Cowan University, Joondalup 6027 WA, Australia*; orcid.org/0000-0002-8080-1590

Alireza Keshavarz − *Discipline of Petroleum Engineering, School of Engineering, Edith Cowan University, Joondalup 6027 WA, Australia*; orcid.org/0000-0002-8091-961X

Muhammad Ali − *Discipline of Petroleum Engineering, School of Engineering, Edith Cowan University, Joondalup 6027 WA, Australia*; orcid.org/0000-0002-2446-3072

Complete contact information is available at: https://pubs.acs.org/10.1021/acsomega.1c07182

Notes

The authors declare no competing financial interest.

■ ACKNOWLEDGMENTS

The authors would like to acknowledge the Petroleum University of Technology (P.U.T) for its support and funding this study through the research grant. The authors also would like to appreciate the Shahriari laboratory center located in Abadan Institute of Technology for providing access to the required laboratory equipment.

■ NOMENCLATURE

EOR	enhanced oil recovery
CEOR	chemical enhanced oil recovery
NEOR	nanotechnology-assisted enhanced oil recovery
RF	recovery factor
IFT	interfacial tension
CMC	critical micelle concentration
CP	Cyclamen persicum
MMT	montmorillonite
ZSC	Ziziphus spina-christi
DDW	double-deionized water
TGA	thermogravimetric analysis
FT-IR	Fourier transform infrared spectroscopy
XRD	X-ray diffraction analysis
FE-SEM	field-emission scanning electron microscopy
PV	pore volume

■ REFERENCES

(1) Saira, S.; Yin, H.; Le-Hussain, F. Effect of Alcohol-Treated CO_2 On Interfacial Tension Between CO_2 and Oil, And Oil Swelling. *Adv. Geo-Energy Res.* **2021-6069**, *5*, 407−421.

(2) Bahraminejad, H.; Manshad, A. K.; Keshavarz, A. Characterization, micellization behavior, and performance of a novel surfactant

https://doi.org/10.1021/acsomega.1c07182
ACS Omega 2022, 7, 24951−24972

derived from Gundelia tournefortii plant during chemical enhanced oil recovery. *Energy Fuels* **2021**, *35*, 1259−1272.
(3) Saira, S.; Janna, F.; Le-Hussain, F. Effectiveness of modified CO_2 injection at improving oil recovery and CO_2 storage-Review and simulations. *Energy Rep.* **2020**, *6*, 1922−1941.
(4) Saira, S.; Ajoma, E.; Le-Hussain, F. A Laboratory Investigation of the Effect of Ethanol-Treated Carbon Dioxide Injection On Oil Recovery and Carbon Dioxide Storage. *SPE J.* **2021**, *26*, 3119−3135.
(5) Nowrouzi, I.; Mohammadi, A. H.; Manshad, A. K. Characterization and Evaluation of a Natural Surfactant Extracted from Soapwort Plant for Alkali-Surfactant-Polymer (ASP) Slug Injection into Sandstone Oil Reservoirs. *J. Mol. Liq.* **2020**, *318*, 114369.
(6) Bahraminejad, H.; Manshad, A. K.; Iglauer, S.; Keshavarz, A. NEOR Mechanisms and Performance Analysis in Carbonate/Sandstone Rock Coated Microfluidic Systems. *Fuel* **2022**, *309*, 122327.
(7) He, Y.; Liao, K.; Bai, J.; Fu, L.; Ma, Q.; Zhang, X.; Ren, Z.; Wang, W. Study on a nonionic surfactant/nanoparticle composite flooding system for enhanced oil recovery. *ACS Omega* **2021**, *6*, 11068−11076.
(8) Almahfood, M.; Bai, B. The Synergistic Effects of Nanoparticle-Surfactant Nanofluids in EOR Applications. *J. Pet. Sci. Eng.* **2018**, *171*, 196−210.
(9) Asl, H. F.; Zargar, G.; Manshad, A. K.; Takassi, M. A.; Ali, J. A.; Keshavarz, A. Effect of SiO_2 Nanoparticles On the Performance of L-Arg and L-Cys Surfactants for Enhanced Oil Recovery in Carbonate Porous Media. *J. Mol. Liq.* **2020**, *300*, 112290.
(10) Sun, X.; Zhang, Y.; Chen, G.; Gai, Z. Application of Nanoparticles in Enhanced Oil Recovery: A Critical Review of Recent Progress. *Energies* **2017**, *10*, 345.
(11) Chhetri, A. B.; Watts, K. C.; Rahman, M. S.; Islam, M. R. Soapnut Extract as A Natural Surfactant for Enhanced Oil Recovery. *Energy Sources, Part A* **2009**, *31*, 1893−1903.
(12) Pordel Shahri, M.; Shadizadeh, S. R.; Jamialahmadi, M. A New Type of Surfactant for Enhanced Oil Recovery. *Pet. Sci. Technol.* **2012**, *30*, 585−593.
(13) Deymeh, H.; Shadizadeh, S. R.; Motafakkerfard, R. Experimental investigation of Seidlitzia rosmarinus effect on oil-water interfacial tension: Usable for chemical enhanced oil recovery. *Sci. Iran.* **2012**, *19*, 1661−1664.
(14) Ahmadi, M. A.; Arabsahebi, Y.; Shadizadeh, S. R.; Shokrollahzadeh Behbahani, S. Preliminary Evaluation of Mulberry Leaf-Derived Surfactant On Interfacial Tension in an Oil-Aqueous System: EOR Application. *Fuel* **2014**, *117*, 749−755.
(15) Rahmati, M.; Mashayekhi, M.; Songolzadeh, R.; Daryasafar, A. Effect of Natural Leaf-Derived Surfactants On Wettability Alteration and Interfacial Tension Reduction in Water-Oil System: EOR Application. *J. Jpn. Pet. Inst.* **2015**, *58*, 245−251.
(16) Emadi, S.; Shadizadeh, S. R.; Manshad, A. K.; Rahimi, A. M.; Mohammadi, A. H. Effect of Nano Silica Particles On Interfacial Tension (IFT) And Mobility Control of Natural Surfactant (Cedr Extraction) Solution in Enhanced Oil Recovery Process by Nano - Surfactant Flooding. *J. Mol. Liq.* **2017**, *248*, 163−167.
(17) Xu, D.; Kang, W.; Zhang, L.; Jiang, J.; Li, Z.; Lu, Y.; Zhang, P.; Wu, H. Ultra-Low Interfacial Tension of a Surfactant Under a Wide Range of Temperature and Salinity Conditions for Chemical Enhanced Oil Recovery. *Tenside, Surfactants, Deterg.* **2018**, *55*, 252−257.
(18) Cheraghian, G.; Kiani, S.; Nassar, N. N.; Alexander, S.; Barron, A. R. Silica Nanoparticle Enhancement in The Efficiency of Surfactant Flooding of Heavy Oil in A Glass Micromodel. *Ind. Eng. Chem. Res.* **2017**, *56*, 8528−8534.
(19) Haeri, F.; Rao, D. N. Precise Wettability Characterization of Carbonate Rocks to Evaluate Oil Recovery Using Surfactant-Based Nanofluids. *Energy Fuels* **2019**, *33*, 8289−8301.
(20) Songolzadeh, R.; Moghadasi, J. Stabilizing Silica Nanoparticles in High Saline Water by Using Ionic Surfactants for Wettability Alteration Application. *Colloid Polym. Sci.* **2016**, *295*, 145−155.
(21) Zhao, M.; Lv, W.; Li, Y.; Dai, C.; Wang, X.; Zhou, H.; Zou, C.; Gao, M.; Zhang, Y.; Wu, Y. Study On the Synergy Between Silica Nanoparticles and Surfactants for Enhanced Oil Recovery During Spontaneous Imbibition. *J. Mol. Liq.* **2018**, *261*, 373−378.
(22) Zhong, X.; Li, C.; Li, Y.; Pu, H.; Zhou, Y.; Zhao, J. X. Enhanced Oil Recovery in High Salinity and Elevated Temperature Conditions with A Zwitterionic Surfactant and Silica Nanoparticles Acting in Synergy. *Energy Fuels* **2020**, *34*, 2893−2902.
(23) Suleimanov, B. A.; Ismailov, F. S.; Veliyev, E. F. Nanofluid for Enhanced Oil Recovery. *J. Pet. Sci. Eng.* **2011**, *78*, 431−437.
(24) Mohajeri, M.; Hemmati, M.; Shekarabi, A. S. An experimental study on using a nanosurfactant in an EOR process of heavy oil in a fractured micromodel. *J. Pet. Sci. Eng.* **2015**, *126*, 162−173.
(25) Shadizadeh, S. S.; Kharrat, R. Experimental Investigation ofMatricaria chamomillaExtract Effect on Oil-Water Interfacial Tension: Usable for Chemical Enhanced Oil Recovery. *Pet. Sci. Technol.* **2015**, *33*, 901−907.
(26) Daghlian Sofla, S. J.; Sharifi, M.; Hemmati Sarapardeh, A. Toward Mechanistic Understanding of Natural Surfactant Flooding in Enhanced Oil Recovery Processes: The Role of Salinity, Surfactant Concentration and Rock Type. *J. Mol. Liq.* **2016**, *222*, 632−639.
(27) Betancur, S.; Carrasco-Marín, F.; Pérez-Cadenas, A. F.; Franco, C. A.; Jiménez, J.; Manrique, E. J.; Quintero, H.; Cortés, F. B. Effect of Magnetic Iron Core-Carbon Shell Nanoparticles in Chemical Enhanced Oil Recovery for Ultralow Interfacial Tension Region. *Energy Fuels* **2019**, *33*, 4158−4168.
(28) Betancur, S.; Giraldo, L. J.; Carrasco-Marín, F.; Riazi, M.; Manrique, E. J.; Quintero, H.; García, H. A.; Franco-Ariza, C. A.; Cortés, F. B. Importance of the Nanofluid Preparation for Ultra-Low Interfacial Tension in Enhanced Oil Recovery Based on Surfactant-Nanoparticle-Brine System Interaction. *ACS Omega* **2019**, *4*, 16171−16180.
(29) Nwidee, L. N.; Lebedev, M.; Barifcani, A.; Sarmadivaleh, M.; Iglauer, S. Wettability Alteration of Oil-Wet Limestone Using Surfactant-Nanoparticle Formulation. *J. Colloid Interface Sci.* **2017**, *504*, 334−345.
(30) Al-zuabe, M. a.; Ismail, Y.; Hasan, D.; Alhrout, H.; Al-Zeidaneen, S.; Albawarshi, Y.; Abu-Hamra, E. Antimicrobial Effect of Cyclamen Persicum Tuber Extracts Against Bacteria and Candida Species. *J. Pure Appl. Microbiol.* **2019**, *13*, 107−116.
(31) Hussen, F. M. A. Activated carbon from Cyclamen Persicum Tubers for Diclofenac removal from aqueous solution. Master's dissertation, An-Najah National University, Nablus, Palestine, 2013.
(32) Jodeh, S.; Abdelwahab, F.; Jaradat, N.; Warad, I.; Jodeh, W. Adsorption of diclofenac from aqueous solution using *Cyclamen persicum* tubers based activated carbon (CTAC). *Journal of the Association of Arab Universities for Basic and Applied Sciences* **2016**, *20*, 32−38.
(33) Jaradat, N. A.; Abualhasan, M.; Ali, I. Comparison of Anti-Oxidant Activities and Exhaustive Extraction Yields Between Wild and Cultivated Cyclamen Persicum, Malva Sylvestris and Urtica Pilulifera Leaves. *J. Appl. Pharmaceut. Sci.* **2015**, *5*, 101−106.
(34) Sani, H. A.; Ahmad, M. B.; Hussein, M. Z.; Ibrahim, N. A.; Musa, A.; Saleh, T. A. Nanocomposite Of Zno With Montmorillonite For Removal Of Lead And Copper Ions From Aqueous Solutions. *Process Saf. Environ. Prot.* **2017**, *109*, 97−105.
(35) Maham, M.; Nasrollahzadeh, M.; Mohammad Sajadi, S. Facile Synthesis of Ag/ZrO_2 Nanocomposite as A Recyclable Catalyst for The Treatment of Environmental Pollutants. *Compos. B Eng.* **2020**, *185*, 107783.
(36) Arashiro, E. Y.; Demarquette, N. R. Use of The Pendant Drop Method to Measure Interfacial Tension Between Molten Polymers. *Mater. Res.* **1999**, *2*, 23−32.
(37) Shahrabadi, A.; Bagherzadeh, H.; Roustaei, A.; Golghanddashti, H. *Experimental Investigation of HLP Nanofluid Potential to Enhance Oil Recovery: A Mechanistic Approach. All Days*; OnePetro, 2012.
(38) Mousavi Moghadam, A.; Baghban Salehi, M. Enhancing Hydrocarbon Productivity Via Wettability Alteration: A Review On the Application of Nanoparticles. *Rev. Chem. Eng.* **2018**, *35*, 531−563.

https://doi.org/10.1021/acsomega.1c07182
ACS Omega 2022, 7, 24951−24972

(39) Talal, J. H.; Mohammed, D. B.; Jawad, K. H. Fabrication of Hydrophobic Nanocomposites Coating Using Electrospinning Technique for Various Substrate. *J. Phys. Conf.* **2018**, *1032*, 012033.
(40) Samal, K.; Das, C.; Mohanty, K. Eco-Friendly Biosurfactant Saponin for The Solubilization of Cationic and Anionic Dyes in Aqueous System. *Dyes Pigm.* **2017**, *140*, 100−108.
(41) Almutairi, M. S.; Ali, M. Direct Detection of Saponins in Crude Extracts of Soapnuts by FTIR. *Nat. Prod. Res.* **2014**, *29*, 1271−1275.
(42) Li, R.; Wu, Z. L.; Wang, Y. J.; Li, L. L. Separation of Total Saponins from The Pericarp of Sapindus Mukorossi Gaerten. By Foam Fractionation. *Ind. Crops Prod.* **2013**, *51*, 163−170.
(43) Tehrani, M. M.; Molahasani, N.; Aghabeygi, S. Sonosynthesis and characterization of nano ZnO/Montmorillonite nano clay composite via Sol-Gel method. *Int. J. Bio-Inorg. Hybr. Nanomater.* **2016**, *5*, 167−172.
(44) Chakraborty, T.; Chakraborty, A.; Shukla, M.; Chattopadhyay, T. ZnO-Bentonite nanocomposite: an efficient catalyst for discharge of dyes, phenol and Cr(VI) from water. *J. Coord. Chem.* **2019**, *72*, 53−68.
(45) Xiong, G.; Pal, U.; Serrano, J. G.; Ucer, K. B.; Williams, R. T. Photoluminesence and FTIR Study of ZnO Nanoparticles: The Impurity and Defect Perspective. *Phys. Status Solidi C* **2006**, *3*, 3577−3581.
(46) Ravi, S. G.; Shadizadeh, S. R.; Moghaddasi, J. Core Flooding Tests to Investigate the Effects of IFT Reduction and Wettability Alteration On Oil Recovery: Using Mulberry Leaf Extract. *Pet. Sci. Technol.* **2015**, *33*, 257−264.
(47) Pal, N.; Saxena, N.; Divya Laxmi, K. V.; Mandal, A. Interfacial Behaviour, Wettability Alteration and Emulsification Characteristics of a Novel Surfactant: Implications for Enhanced Oil Recovery. *Chem. Eng. Sci.* **2018**, *187*, 200−212.
(48) Onsager, L. Deviations from Ohm's Law in Weak Electrolytes. *J. Chem. Phys.* **1934**, *2*, 599−615.
(49) Kumar, A.; Mandal, A. Synthesis and Physiochemical Characterization of Zwitterionic Surfactant for Application in Enhanced Oil Recovery. *J. Mol. Liq.* **2017**, *243*, 61−71.
(50) Nowrouzi, I.; Mohammadi, A. H.; Manshad, A. K. Water-Oil Interfacial Tension (IFT) Reduction and Wettability Alteration in Surfactant Flooding Process Using Extracted Saponin from Anabasis Setifera Plant. *J. Pet. Sci. Eng.* **2020**, *189*, 106901.
(51) Buckley, J. S.; Liu, Y.; Monsterleet, S. Mechanisms of Wetting Alteration by Crude Oils. *SPE J.* **1998**, *3*, 54−61.
(52) Jarrahian, K.; Seiedi, O.; Sheykhan, M.; Sefti, M. V.; Ayatollahi, S. Wettability Alteration of Carbonate Rocks by Surfactants: A Mechanistic Study. *Colloids Surf., A* **2012**, *410*, 1−10.
(53) Benabid, F.; Kharchi, N.; Zouai, F.; Mourad, A.-H. I.; Benachour, D. Impact of Co-Mixing Technique and Surface Modification of Zno Nanoparticles Using Stearic Acid On Their Dispersion into HDPE to Produce HDPE/Zno Nanocomposites. *Polym. Polym. Compos.* **2019**, *27*, 389−399.
(54) Nazarahari, M. J.; Manshad, A. K.; Ali, M.; Ali, J. A.; Shafiei, A.; Sajadi, S. M.; Moradi, S.; Iglauer, S.; Keshavarz, A. Impact of A Novel Biosynthesized Nanocomposite (Sio2@Montmorilant@Xanthan) On Wettability Shift and Interfacial Tension: Applications for Enhanced Oil Recovery. *Fuel* **2021**, *298*, 120773.
(55) Lau, H. C.; Yu, M.; Nguyen, Q. P. Nanotechnology for Oilfield Applications: Challenges and Impact. *J. Pet. Sci. Eng.* **2017**, *157*, 1160−1169.
(56) Dolai, J.; Mandal, K.; Jana, N. R. Nanoparticle Size Effects in Biomedical Applications. *ACS Appl. Nano Mater.* **2021**, *4*, 6471−6496.
(57) Chengara, A.; Nikolov, A. D.; Wasan, D. T.; Trokhymchuk, A.; Henderson, D. Spreading of Nanofluids Driven by The Structural Disjoining Pressure Gradient. *J. Colloid Interface Sci.* **2004**, *280*, 192−201.
(58) Manshad, A. K.; Ali, J. A.; Haghighi, O. M.; Mohammad Sajadi, S.; Keshavarz, A. Oil Recovery Aspects Of Zno/Sio2 Nano-Clay In Carbonate Reservoir. *Fuel* **2022**, *307*, 121927.
(59) Mcelfresh, P.; Olguin, C.; Ector, D. *The Application of Nanoparticle Dispersions to Remove Paraffin and Polymer Filter Cake Damage. All Days*; OnePetro, 2012.
(60) Bahraminejad, H.; Khaksar Manshad, A.; Riazi, M.; Ali, J. A.; Sajadi, S. M.; Keshavarz, A. CuO/TiO_2/PAM as a Novel Introduced Hybrid Agent for Water-Oil Interfacial Tension and Wettability Optimization in Chemical Enhanced Oil Recovery. *Energy Fuels* **2019**, *33*, 10547−10560.
(61) Meng, X. W.; Li, Y.; Shen, L.; Yang, X. Q. Reinforcing A Water Bridge in A Disjoint Nanochannel. *Europhys. Lett.* **2020**, *131*, 20003.
(62) Horozov, T. S.; Aveyard, R.; Clint, J. H.; Binks, B. P. Order−Disorder Transition in Monolayers of Modified Monodisperse Silica Particles at the Octane−Water Interface. *Langmuir* **2003**, *19*, 2822−2829.
(63) Conn, C. A.; Ma, K.; Hirasaki, G. J.; Biswal, S. L. Visualizing Oil Displacement with Foam in A Microfluidic Device with Permeability Contrast. *Lab Chip* **2014**, *14*, 3968−3977.
(64) Majidaie, S.; Muhammad, M.; Tan, I.; Demiral, B. Green Surfactant for Enhanced Oil Recovery. *2011 National Postgraduate Conference*, 2011.

https://doi.org/10.1021/acsomega.1c07182
ACS Omega 2022, 7, 24951−24972